https://doi.org/10.5194/egusphere-2025-2006
Preprint. Discussion started: 14 May 2025

Parent material geochemistry – and not plant input - as the primary element shaping soil organic carbon stocks in European alpine grasslands

Annina Maier[1,*], Maria, E. Macfarlane[1, 2,*], Marco Griepentrog[1], and Sebastian Doetterl[1]

[1]Department of Environmental Systems Science, Swiss Federal Institute of Technology (ETH) Zurich, 8092 Zurich, Switzerland
[2]Department of Civil and Environmental Engineering, Massachusetts Institute of Technology (MIT), 02139-4307 Cambridge, MA, USA
[*]These authors contributed equally to this work.

Correspondence: Annina Maier (annina.maier@usys.ethz.ch)

Abstract. Soils represent the largest terrestrial carbon (C) reservoir on Earth. Within terrestrial ecosystems, soil geochemistry can be a strong driver of plant-soil-carbon dynamics, especially in young, less weathered soils. Here, we investigate the impact of potential plant biomass input, soil fertility parameters, and soil organic carbon (SOC) stabilization mechanisms on the distribution of SOC in European alpine grasslands across gradients of geochemically distinct parent materials. We demonstrate that SOC stock accrual in geochemically young, developing alpine soils is dependent on soil mineralogy as a result of parent material weathering, and is not strongly linked to plant biomass input. We show potential differences in the importance of SOC stabilization mechanisms, with universally large relative contributions ($\geq$ 50 %) of the microaggregate soil fraction to bulk SOC. We further show that concentrations of Fe, Al and Mn pedogenic oxides coincide with SOC stock magnitude across an alpine soil geochemical gradient, where SOC stocks range between 8.1–23.2 kg C m^{-2}. Our results highlight that soil fertility, which governs plant C inputs, and soil mineralogical characteristics, which control C stabilization, play equally crucial roles in predicting SOC contents in alpine soils at an early development stage, corroborated by soil fraction modern ($F^{14}C$) values ranging from 0.77–1.06.

1 Introduction

Mountain ecosystems are experiencing intense climate warming with temperatures increasing by 0.4–0.6 °C per decade (Pepin et al., 2015; Vitasse et al., 2021). This warming may result in the extension of vegetation zones and thermal limits of plant life by 300–600 m in elevation (Hagedorn et al., 2019). Indeed, an increase in alpine plant productivity has already been detected in mountains of central Asia and the European Alps (Choler et al., 2021; Anderson et al., 2020; Carlson et al., 2017). Approximately 77 % of the area of European Alps has experienced greening above the treeline within the last four decades alone.

https://doi.org/10.5194/egusphere-2025-2006
Preprint. Discussion started: 14 May 2025

However, while many studies have focused on the responses of aboveground mountain vegetation to climate warming (Rumpf et al., 2022; Nomoto and Alexander, 2021; Steinbauer et al., 2018), less attention has been given to belowground changes and the impact of ongoing soil weathering, despite more than 90 % of alpine ecosystem carbon (C) being stored in soils above the treeline (Körner, 2003). In this regard, climate's interaction with parent material and geochemistry are important factors governing rates of soil weathering and remain understudied controls on C cycling and stabilization in alpine soils (Jenny, 1994; Barré et al., 2017; Yang et al., 2020).

Plants residues represent the main source of organic carbon (OC) entering the soil system. The extent of this input depends on variations in above- and belowground biomass production, which are influenced by climate zone, elevation and soil parent material (Körner, 2003; Hagedorn et al., 2019; O'Sullivan et al., 2020; Augusto et al., 2017; Paoli et al., 2008). Through weathering processes, parent material delivers nutrients into the soil solution, which are a limiting factor for plant growth, especially in young alpine ecosystems (Möhl et al., 2019; Körner, 2003). Weathering also leads to increased formation of reactive secondary minerals, such as expandable clays. Together with cations they contribute to SOC stabilization and persistence through direct interaction and complexation of organic molecules, a mechanism which is highly influenced by parent material geochemistry and soil weathering (Rowley et al., 2018; Solly et al., 2020). SOC persistence is further promoted by aggregate formation and stability, which are enhanced by clay content, Ca^{2+} ions (in high pH soils), and pedogenic oxy(hydr-)oxides (Olagoke et al., 2022; Rowley et al., 2021; Kirsten et al., 2021). Recent studies highlight pedogenic Fe and Al oxy(hydr-)oxides as key drivers of SOC stabilization, often surpassing silicate clay minerals in importance (Fang et al., 2021; Doetterl et al., 2015; Mao et al., 2020; Yang et al., 2020; Kirsten et al., 2021; Reichenbach et al., 2021). Their poorly crystalline forms enhance aggregation (Baldock and Skjemstad, 2000; Duiker et al., 2003; Kaiser et al., 2016) and provide reactive surfaces for SOC stabilization via ligand exchange (Lützow et al., 2006).

Climate warming will induce an acceleration in soil weathering rates and improve climatic growth conditions of high-altitude vegetation, which may also lead to the development of larger SOC stocks (Rumpf et al., 2022; Muñoz et al., 2023). The rate and extent to which climatic change may influence the soil matrix and long-term SOC stabilization is strongly linked to the reactivity of the soil's mineral phase, which is largely governed by parent material (Doetterl et al., 2015). The majority of past work on the future of the alpine soil C cycle has focused on studying elevational SOC gradients studying vegetation patterns (Hitz et al., 2001; Guidi et al., 2024) as well as soil parameters in relation to different alpine habitats (Canedoli et al., 2020; Cao et al., 2013). A systematic analysis of the interaction between the pedosphere and biosphere in shaping regional-scale alpine SOC stocks across geochemically contrasting parent materials remains missing. Exploring variations in soil weathering, biomass inputs, and SOC stocks across different parent materials will likely improve our understanding of future C cycling in alpine environments. Accordingly, we examine soils formed on five geochemically distinct parent materials (Dolomite, Flysch, Gneiss, Greenschist, Marl) in the European Alps to assess how differences in parent material—and consequently soil geochemistry—influence (i) the magnitude and variability of potential biomass inputs (above- and belowground) and (ii) SOC stocks. To do so, we pair the quantification of SOC stocks under comparable climatic and environmental condition with an assessment

https://doi.org/10.5194/egusphere-2025-2006
Preprint. Discussion started: 14 May 2025

of the persistence of soil C, via radiocarbon (^{14}C) analyses and how different soil stabilization mechanisms contribute to bulk SOC, via physical soil fractionation.

First, we hypothesize that i) soils developed on nutrient-rich parent materials will exhibit the highest biomass inputs and potentially also the highest overall SOC stocks, if soils can stabilize these inputs (e.g. through high clay or iron content). We expect this for soils developed e.g. on Marl or Greenschist, as they have a high mineral weatherability, supplying an elevated amount of reactive clay-sized minerals for mineral C stabilization and the build-up of a porous soil matrix. More specifically, we expect that ii) soils with a higher amount of pedogenic oxides - and not the amount of clay as a particle size - will lead to greater SOC stocks, because of the stabilization potential of those minerals (Rasmussen et al., 2018). This will most likely be the case for the soils developed on mafic and siliceous, rocks (i.e., Greenschist and Gneiss) which are rich in Fe, Al and manganese (Mn) in contrast to soils developed from carbonatic (Marl, Dolomite) parent material. Lastly, we expect iii) soils that are more strongly weathered will not only show higher SOC stocks but also older ^{14}C values, hinting at higher persistence, as SOC is better protected (more persistent against microbial decomposition) in these soils. We rationalize this with the fact that these soils have developed a wider portfolio of efficient mineral-related stabilization mechanisms (occlusion of C within microaggregates and protection through association with minerals in contrast to C being present as free particulate organic matter) (Kleber et al., 2015; Torn et al., 2013).

2 Materials and methods

2.1 Study area

The study area was located within grasslands and meadows of the European Alps, along a geochemical gradient of soil parent materials. Three out of five suitable study sites with Flysch, Gneiss, and Greenschist as parent materials were located in the Eastern part of Switzerland (i.e., canton of Graubünden). The two remaining study sites with Dolomite and Marl as parent materials were sampled in Germany and Austria, respectively (Fig. 1). The specific sampling sites were chosen based on geological maps (Federal Office of Topography swisstopo, 2020; Federal Institute of Geosciences and Natural Resources, 2020) (Fig. 1). Sampling sites varied primarily in parent material while elevation, aspect, and climatic factors were kept as constant as possible. The elevation of all sampling sites is within a range of 2000–2300 m a.s.l. There was little variation in climate among the sites. The mean annual temperature (MAT) of the sites ranges between 1.4–2.8 °C (Hagedorn et al., 2010; Bassin et al., 2013) and the mean annual precipitation (MAP) varied from a minimum of 1050 mm in Davos (CH) to a maximum of 1300 mm in the Zugspitze region (DE) and in Allgäu (AT) (VAO (Virtual Alpine Observatory), 2020). A more detailed description of the sampling sites' locations as well as their geochemical and climatic characteristics are summarized in Table 1.

All examined parent materials are distinct in their geochemical composition and formed clearly distinguishable soils (Table 1, Fig. 2). To classify each sampling site's soil type, soil profiles were dug in the center of the sampling plots and described according to the Manual of Soil Mapping (Eckelmann et al., 2006). Soil classification was done following the World Reference

https://doi.org/10.5194/egusphere-2025-2006
Preprint. Discussion started: 14 May 2025

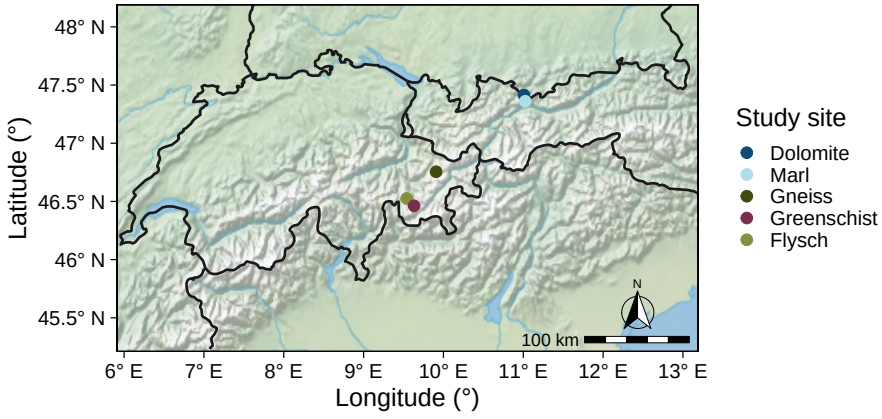

Figure 1. Locations of the soil sampling sites developed on distinct parent materials. This map was created using Natural Earth.

Base for Soil Resources (WRB, 2015). The soil developed on Dolomite was classified as a dolomitic Leptosol. This soil did not possess any mineral horizons but had an average 12.9 ± 2.2 cm thick Oh horizon, which was lacking in all other sites' profiles. The Dolomite site's Oh horizon lies directly on top of the bedrock (R) horizon, which consists of carbonatic material. All other sites developed Ah and Bw horizons of varying thicknesses on top of a Cw horizon. The soil developed on Flysch reached a depth of 37.2 ± 0.2 cm and was classified as an argic Umbrisol. The soil on Gneiss developed 53.7 ± 1.8 cm as a spodic Umbrisol, due to the accumulation of Fe and Al oxides in subsurface horizons. The soil on Greenschist developed into 39.9 ± 3.2 cm depth as an Umbrisol. The soil on Marl developed into 67.2 ± 1.2 cm depth as a calcic Cambisol, containing some carbonatic material in its Cw horizon. The rooting depths of all sites reached until at least the end of their Bw horizons, except the Gneiss site which reached approximately half of the Bw horizon depth. Further information on the examined soils' biogeochemical and physical characteristics can be found in Table 4.

2.2 Sampling design

Soil and biomass sampling was carried out during the vegetation growth period from late June to early September in 2020. At each site, four field replicate plots of 25 x 25 m were chosen. The plots were considered suitable when their slopes were between 40 %–60 %, their aspects were south-facing (with slight variation across sampling sites from SE to SW), and no troughs were found. Ten soil monoliths were sampled per field replicate plot in a depth-explicit way, respecting horizon boundaries and with the aim of reaching the least weathered horizon (C horizon) at each sampling site. Each horizon of the soil monoliths was sampled using a Kopecky cylinder. Then, the ten soil samples sampled by Kopecky cylinders per horizon and plot were merged into one composite sample per field replicate plot. Additionally, an Edelman auger was used to obtain samples of the weathered bedrock (Cw) and of the parent material, i.e., unweathered bedrock (R). Further, at each field replicate plot five smaller plots were chosen as representative field replicates for aboveground plant biomass sampling. Each of these replicates covered an area of 0.2 x 0.2 m for the Marl and Flysch sites and 0.4 x 0.4 m for the Gneiss, Greenschist and Dolomite sites. From these

https://doi.org/10.5194/egusphere-2025-2006
Preprint. Discussion started: 14 May 2025

Table 1. Overview on parent materials, geochemical characteristics, locations, elevation ranges, MAT and MAP of the study sites.

Parent material	Geochemical characteristics	Location	Elevation (m.s.l.)	MAT (°C)	MAP (mm)
Dolomite	Carbonatic	Wettersteinkalk mountain range (DE)	2000–2300	1.4	1300
Marl	Carbonatic, sedimentary	Allgäu Alps (AT)	2180–2230	1.4	1300
Gneiss	Siliceous, intermediate metamorphic	Dischma valley, Davos (CH)	2080–2200	1.4	1050
Greenschist	Siliceous, mafic metamorphic, Mg-rich	Crap da Radons, Bivio (CH)	2160–2200	2.8	1200
Flysch	Siliceous, intermediate sedimentary	Curtegns valley, Savognin (CH)	2180–2220	2.8	1200

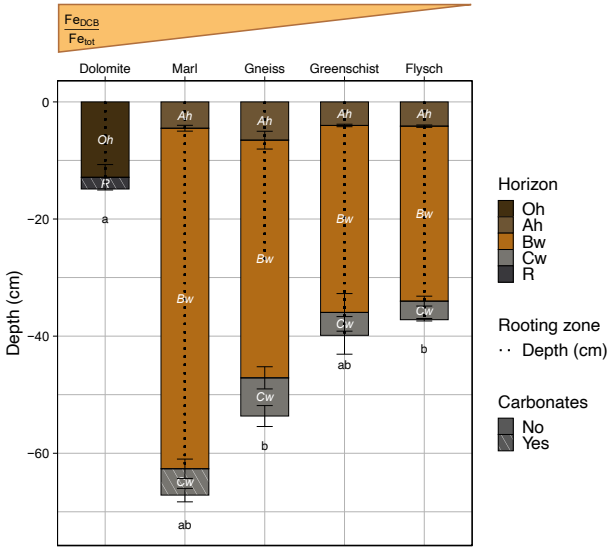

Figure 2. Average total depth of whole soil profiles, divided into individual horizons (cm), average rooting depth (cm) and presence of carbonates (No/Yes) are shown ± standard errors, across all sites. Soil profiles are displayed along a relative gradient in Fe_{DCB}/Fe_{tot}. Precise values for these indices per soil horizon can be found in Table 4. A description and the calculation of this index can be found in Sect. 2.3.6. Note that the Dolomite site's Oh horizon is an organic horizon, however it is displayed in a similar fashion to all other mineral horizons for illustrative purposes. Same respective lowercase letters denote total soil profile development depths, that are not statistically significant from one another.

smaller plots, the entire aboveground biomass was sampled. Ultimately across all five study sites a total of 100 observations were sampled, consisting of 46 soil, 18 parent material, 18 above- and 18 belowground plant biomass samples.

https://doi.org/10.5194/egusphere-2025-2006
Preprint. Discussion started: 14 May 2025

2.3 Laboratory analyses

2.3.1 Sample processing

All collected soil and aboveground biomass samples were oven-dried at 40 °C for 96 h and their dry weights noted. Total aboveground plant biomass was then split into woody vs. non-woody biomass and their respective weights noted. Dried soil samples were split and sieved through a 2 mm sieve. Large roots that did not pass through the 2 mm mesh were collected and weighed. Fine roots that passed the 2 mm mesh were collected with tweezers. The fine soil fraction (< 2 mm) gained from sieving was used for further analyses. Moreover, an aliquot of each fine soil sample was powder-milled (Mixer Mill MM 200, Retsch GmbH Haan, Germany) as a requirement for certain analyses such as carbon (C) and nitrogen (N) contents, elemental composition, bioavailable phosphorus, cation exchange capacity, sequential pedogenic oxide extraction and ^{14}C analyses. Further, a representative aliquot of each site's aboveground plant biomass was homogenized in two steps for C and N analyses; the plant material was coarsely shredded in a blender and then powder-milled. In addition, a representative aliquot of each site's belowground biomass (coarse and fine roots) was powder-milled (Mixer Mill MM 200, Retsch GmbH Haan, Germany).

2.3.2 Physical soil fractionation

Physical fractionation of bulk soil samples was conducted on three of the four field replicates per sampling site, with the exception of the Marl site. For this site only two of the four field replicate plots were included in the physical fractionation scheme. The respective excluded sampling plots displayed a parent material geochemistry that did not correspond with the geochemical composition of a typical Marl, exhibiting markedly higher Si contents. These correspond to the same plots that were included for statistical analyses (see details in Sect. 2.3.8). The fractionation corresponded to a simplified version of Six et al. (2000), as applied in Doetterl et al. (2018) using a microaggregate isolator installed on a sample shaker. First, a 20 g aliquot of bulk soil samples (< 2 mm) was weighed and submerged in water for 48 h to break down non-water-stable aggregates. Second, the samples were wet-sieved through a 250 µm sieve, with the material > 250 µm building the coarse particulate organic matter (POM) fraction. Macroaggregates were broken up using the microaggregate isolator and shaker. Subsequently, samples were sieved through a 53 µm sieve to obtain the silt and clay (s+c) fraction (< 53 µm) and the stable microaggregate fraction (MA) (53–250 µm). Finally, the obtained fractions were analyzed for their N and OC content (Sect. 2.3.4). The procedural and conceptual interpretations of the obtained fractions can be found in Table 2. An overview on the fractionation results can be found in Table A1.

2.3.3 Determination of soil texture, pH, elemental composition and effective cation exchange capacity

Soil texture was determined according to Miller and Schaetzl (2012) using a laser diffraction particle size analyzer (LS 13 320 Laser Diffraction Particle Size Analyzer, Beckman Coulter, Brea, CA, United States). For the pH measurement, 15 ml of 0.01 M $CaCl_2$ was added to 3 g of soil sample. The samples were shaken horizontally for 10 minutes and measured after 24

https://doi.org/10.5194/egusphere-2025-2006
Preprint. Discussion started: 14 May 2025

Table 2. Fraction names and abbreviations, procedural definitions and conceptual interpretations of SOC associated with the respective soil fractions. This table was adapted from Doetterl et al. (2018) and Doetterl et al. (2015).

Fraction	Procedural definition	Conceptual SOC interpretation
Coarse particulate organic matter (POM)	> 250 µm	Unprotected SOC, non mineral-associated
Stable microaggregates (MA)	53–250 µm	Microaggregate-associated SOC: physical separation of unprotected SOC through aggregation and organo-mineral association
Non-aggregated silt and clay (s+c)	< 53 µm	Non-aggregated silt- and clay-associated SOC: organo-mineral association of SOC and association with smallest aggregates

h with a pH meter (Metrohm 713). X-ray fluorescence (XRF) spectrometry was applied to determine the composition of the heavier elements Si, Ti and Zr (Spectro XEPOS, Spectro Analytical Instruments, Kleve, Germany) in powder-milled fine soil and parent material samples. The elements Na, K, Ca, Mg, Fe, Al and Mn were determined by inductively coupled plasma optical emission spectrometry (ICP-OES) (5100 ICP-OES, Agilent Technologies, Santa Clara, CA, United States). Here for, 1 g of milled fine soil samples were weighed into plastic tubes and were extracted with "aqua regia", i.e. 2 ml nanopure H_2O, 6 ml hydrochloric acid (HCl, 37 %) and 2 ml nitric acid (HNO_3, 65 %) for 150 min at 120 °C. The extracts were then diluted with nanopure H_2O to a defined volume of 50 ml and filtered through 20 µm paper filters. Effective cation exchange capacity (CEC_{eff}) and the amount of exchangeable cations were determined according to Hendershot and Duquette (1986) using $BaCl_2$. Sampling site specific patterns in soil texture, pH and CEC_{eff} can be found in Table 4.

2.3.4 Determination of organic carbon, nitrogen, bioavailable phosphorous content

The aliqouts from the powder-milled, dried fine soil and plant samples mentioned above (Sect. 2.3.1) were analyzed for their OC and N content using a CN analyzer (Vario MAX cube, Elementar, Langenselbold, Germany). Soils with a pH > 6 were measured a second time following carbonate removal, to accurately measure organic carbon contents. Carbonate removal was conducted following Walthert et al. (2010) using hydrochloric acid (HCl) fumigation.

The dry weights of the collected plant and root biomass samples, together with their OC and N contents were used to receive above- and belowground OC stocks and use them as proxies for potential C inputs into the soil (Sect. 2.3.7, Eq. 1). Regarding the choice to mix fine and coarse roots into joined, composite samples, we would like to acknowledge the differences in C:N ratios, decomposition mechanisms and functions that exist between coarse and fine roots (Zhang and Wang, 2015). However, fine root samples constituted only very small fractions of overall belowground plant biomass and our primary objective was to obtain an approximate estimate of respective belowground C and N contents. Further, we acknowledge that this approach does not allow for the separation of living and dead roots at the time of sampling or the assessment of belowground biomass productivity. Lastly, we recognize that the analysis of standing aboveground biomass stocks does not truly represent aboveground

https://doi.org/10.5194/egusphere-2025-2006
Preprint. Discussion started: 14 May 2025

OC inputs into the soil, compared to e.g. quantification of effective litter inputs into the soil. However, it should allow for a snapshot of potential below- vs. maximum aboveground biomass inputs at the time of sampling, which is the main purpose of the data.

For the determination of bioavailable phosphorus (bio-P) content, soil samples were extracted with anion exchange membranes (VWR International, material no. 551642 S) in H_2O for 16 h with a 4 cm^2 membrane per g of fresh soil. Prior to extraction, the membranes were activated with 0.5 M $NaHCO_3$. Post extraction, the P retained on the membranes was extracted off the membranes during 1.5 h on a horizontal shaker by using 0.25 M H_2SO_4. Finally, the P contained in the resulting extracts was quantified with ICP-OES (5100 ICP-OES, Agilent Technologies). Parent material specific patterns in bio-P can be found in Table 4.

2.3.5 Sequential extraction of pedogenic oxides

To identify reactive metal phases that can interact (and potentially stabilized) soil C, Fe, Al and Mn oxides were extracted sequentially using sodium pyrophosphate (PP) (Bascomb, 1968), ammonium oxalate (AO) (Dahlgren, 1994), and dithionite-citrate-bicarbonate (DCB) solutions (Mehra and Jackson, 1958). The extraction procedure is based on duplicate extractions, hence, each sample was extracted twice in the form of two subsamples which were merged for final measurement with ICP-OES (5100 ICP-OES, Agilent Technologies, Santa Clara, CA, United States). We acknowledge that a release of elements from non-target, more crystalline minerals such as magnetite, maghemite, biotite, chlorite, muscovite and illite may occur to varying extent during any of the three sequential extraction steps. To which degree is often unknown prior to extraction (Rennert, 2018). Therefore, the interpretation of pyrophosphate extracts as the organo-metal complexed oxides is treated with caution. The term "pedogenic" oxides for Fe-, Al- and Mn- phases extracted in the context of this extraction procedure, is applied for purposes of simplicity. For clarification, Table 3 provides an overview on how the extractable fractions were interpreted. Site-specific patterns in the sum of Fe, Al and Mn pedogenic oxides, extracted with PP and AO, can be found in Table 4.

Table 3. Abbreviations, definitions and interpretation of extracted Fe, Al, Mn pedogenic oxides following Carter and Gregorich (2008).

Abbreviation	Definition	Interpretation
Fe_{PP}, Al_{PP}, Mn_{PP}	Pyrophosphate-extractable Fe, Al, Mn	Primarily dissolved organo-metal-complexed Fe, Al, Mn oxides but may also include some (<10 %) poorly crystalline oxides
Fe_{AO}, Al_{AO}, Mn_{AO}	Ammonium-oxalate-extractable Fe, Al, Mn	Poorly crystalline Fe, Al, Mn oxides and short-range order minerals
Fe_{DCB}, Al_{DCB}, Mn_{DCB}	DCB-extractable Fe, Al Mn	More crystalline Fe, Al, Mn oxides

https://doi.org/10.5194/egusphere-2025-2006
Preprint. Discussion started: 14 May 2025

2.3.6 Calculation of weathering and fertility indices, determination of $F^{14}C$

Weathering and fertility indices including the total reserve of base cations (TRB) (ΣCa, K, Mg and Na (g kg^{-1})) and the ratio of DCB-extractable Fe to total Fe (Fe_{DCB}/Fe_{tot} (-)) were calculated for each horizon of every sampling site. TRB decreases with ongoing soil development, as these soluble cations are increasingly leached from the soil (Brady and Weil, 2008). The Fe_{DCB}/Fe_{tot} ratio relates total pedogenetially-transformed Fe phases extracted with DCB, to total Fe. This value increases with ongoing soil development as more Fe becomes pedogenetially-transformed to more crystalline oxide forms. These weathering/fertility indices were calculated based on measured values of ICP-OES measurements for TRB and on sequential pedogenic oxide concentrations and ICP-OES measurements for Fe_{DCB}/Fe_{tot}. Site-specific patterns in Fe_{DCB}/Fe_{tot} ratios and TRB can be found in Table 4. Note that while Dolomite is displayed as the site with the highest value for the weathering index Fe_{DCB}/Fe_{tot} (Fig. 2, Table 4), this value does not represent the true value for the in situ Dolomite soil. A past report has shown that most horizons of examined soil profiles in the Wettersteinkalk/Zugspitze region show signs of aeolian influence (Küfmann, 2008). Thus the Fe_{DCB}/Fe_{tot} value found at the Dolomite site rather reflects in situ weathering of deposited mineral dust inputs.

Composite samples of bulk soil for ^{14}C analyses were created by pooling similar masses per horizon of each sites' respective field replicates. From these composites, small subsamples between 2–32 mg of milled material, corresponding to ca. 300 µg C, were transferred into 0.025 ml tin capsules. Prior to measurement with the EA-AMS, samples were acidified to remove carbonates (Komada et al., 2008). ^{14}C analyses were conducted using an elemental analyzer coupled to a gas-ion-source equipped accelerator mass spectrometer (EA-AMS) at the Laboratory of Ion Beam Physics (LIP) at ETH Zurich (Haghipour et al., 2019; Welte et al., 2018). Results of the ^{14}C analysis are reported as fraction modern ($F^{14}C$) according to Reimer et al. (2004). $F^{14}C$ values were compared across sites and soil horizons. The values were interpreted as a proxy of soil persistence and as an indicator of longer term SOC stabilization and turnover dynamics. Hereby, lower $F^{14}C$ values were interpreted as being more persistent, i.e. more stable, than higher $F^{14}C$ values (Mathieu et al., 2015). $F^{14}C$ values > 1 are defined as modern. We acknowledge that the measured bulk ^{14}C values represent a mixture of different C pools with different stabilities/persistence and that these values we report may under- or overestimate soil C persistence (Torn et al., 2013; Trumbore, 2000).

2.3.7 Calculation of plant biomass and soil organic carbon stocks

Plant biomass OC stocks for above- and belowground biomass were calculated based on the plant biomass dry weight (DW) and the OC concentration values for above- and belowground biomass per sampling site. Where plant biomass OC stock (BM OC_{stock_i}) is defined as the plant biomass OC stock for above- or belowground (i) plant biomass following Eq. 1.

$$BM\,OC_{stock_i}\,(kg\,m^{-2}) = BM\,OC_{conc_i}\,(\%) \cdot BM\,DW_i\,(kg\,C\,m^{-2}) \quad (1)$$

The most commonly used method to calculate SOC stocks is based on bulk density, soil horizon thickness, and the SOC concentration values (Poeplau et al., 2017). However, this simple calculation often overestimates SOC stocks because it neglects the rock fragment fraction. Thus, SOC horizon stocks (SOC_{stock_j}) were calculated following Eq. 3 proposed by Poeplau et al.

https://doi.org/10.5194/egusphere-2025-2006
Preprint. Discussion started: 14 May 2025

(2017) where FSS_j is defined as fine soil stock per horizon (j) (Eq. 2) and the volume of rocks is included in the $volume_{sample}$. Whole profile SOC stocks were calculated by summing all horizon specific SOC stocks per sampling site.

$$FSS_j\,(kg\,m^{-2}) = \frac{mass_{finesoil}\,(kg)}{volume_{sample}\,(m^{-3})} \cdot depth_j\,(m) \tag{2}$$

$$SOC_{stock_j}\,(kg\,m^{-2}) = SOC_{conc_{finesoil}}\,(\%) \cdot FSS_j\,(kg\,C\,m^{-2}) \tag{3}$$

2.3.8 Statistical analyses

Data are presented as means of related replicates with standard errors, unless specified otherwise. All statistical analyses were performed in R Studio (Version 2023.09.1+494). One-way ANOVA was used to assess the main effect of site-specific parent materials on above- and belowground plant OC stocks as well as total SOC stocks. In each ANOVA, we tested the null hypothesis that there are no significant differences in OC stocks across the soils developed on different, site-specific parent materials. Tukey's HSD post-hoc tests were conducted to identify specific group differences. Statistical significance was set at a p-value < 0.05. To analyze the effect of site-specific parent materials on aboveground plant organic carbon stocks, we employed a non-parametric alternative, due to the violation of the normality assumption required for ANOVA. Specifically, we conducted a Kruskal-Wallis test to assess the main effect of site-specific parent materials on aboveground plant organic carbon stocks. Then we performed Dunn's post hoc test to identify specific group differences.

In connection to our research hypotheses that i) soils with greater soil fertility, enable better plant growth and potentially higher SOC stock accumulation and ii) soils with a more reactive mineral phase should contribute to greater SOC stabilization, we were interested in which set of parameters underlying these hypotheses could better predict SOC stocks in alpine grasslands. With this in mind, two different, hypothesis-driven SOC prediction models were built and compared to see if one model could outperform the other. For the soil fertility model C:N ratio, clay content, pH value and soil nutrient variables (i.e. bio-P, Mg, Ca) were selected as predictor variables. Soil C:N ratio was included because it reflects the stability/degradability of organic matter and how nutrients, especially N, will cycle through the soil (Havlin et al., 2013). Clay content was included, as their negative and variable charge give them a greater ability to bind to positively charged nutrient ions, contributing to soil fertility and nutrient retention (Kleber et al., 2015). Soil nutrient variables and pH were included as the overall concentration and availability of soil nutrients affects soil fertility (Havlin et al., 2013). For the soil mineralogy model organically-complexed and poorly crystalline Fe, Al, and Mn oxides as well as clay content were selected. These variables were included because of their significant ability to stabilize OC through associations or organo-mineral complexes as a result of their large reactive surface area (Kögel-Knabner and Kleber, 2011; Kleber et al., 2015).

The number of predictor variables was kept < 10 due to limited observation availability ($n = 42$). Prior to predictive modelling, all predictor variables were z-score normalized to avoid any scale bias. A selection of linear and nonlinear regressions

https://doi.org/10.5194/egusphere-2025-2006
Preprint. Discussion started: 14 May 2025

were computed, of which the nonlinear random forest regression was ultimately chosen as the most suitable model (Table B1). The maximum number of trees was constrained to 1000. The random forests' tuning parameter, m_{try}, the number of randomly selected predictors chosen at each split, was set to be one third of the number of total possible predictors (Kuhn and Johnson, 2013; Breiman, 2001). To further mitigate overfitting, the random forest models were cross-validated with 10-fold repeated cross validation, for which every model was trained with 70 % of the data and tested with the remaining 30 %. The random forest regressions were run using the caret package (Kuhn, 2008). For the predictive modelling of SOC stocks, only mineral horizons were included, as organic horizons have distinctly different SOC dynamics (Salomé et al., 2010). Hence, the Dolomite site's samples were excluded.

3 Results

3.1 Characterization of the soil profiles based on soil fertility and soil mineralogical properties

3.1.1 Soil fertility

The widest C:N ratios in average aboveground plant biomass are those of the Gneiss and Greenschist sites (40.7 ± 2.0 vs. 60.8 ± 3.9, respectively) and the narrowest are at the Marl and Flysch sites (27.8 ± 5.4 vs. 25.9 ± 1.0, respectively) (Table 4). The widest C:N ratios in average belowground plant biomass can be found at the Gneiss and Greenschist sites (84.4 ± 12.7 vs. 75.1 ± 2.2, respectively) and the narrowest at the Marl and Flysch sites (33.8 ± 3.7 vs. 30.5 ± 2.2, respectively) again. Bulk soil C:N ratios reflect the trends from the above- and belowground biomass C:N ratios. Thus, the widest average bulk soil C:N ratios can be found at the Gneiss and Greenschist sites (16.1 ± 1.5 vs. 12.2 ± 0.2, respectively) and the lowest at the Marl and Flysch sites (11.2 ± 0.8 vs. 9.7 ± 0.4, respectively). The lowest pH average values can be found at the Gneiss (3.8 ± 0.1) and the highest at the Marl site (5.6 ± 0.8). Bio-P concentrations are highest at the Flysch site, ranging from 50.4–1.1 mg kg^{-1} and lowest at the Greenschist site, ranging from 22.4–0.6 mg kg−1. However, there is no significant difference in bio-P concentrations across sites ($p > 0.05$). Marl and Greenschist's sites have the largest average CEC_{eff} (25.0 ± 2.9 vs. 20.8 ± 1.3 cmol kg^{-1}, respectively) and TRB (33.3 ± 46.2 vs. 20.8 ± 8.3 g kg^{-1}, respectively). The Gneiss site has the lowest average CEC_{eff} (9.9 ± 1.2 cmol kg^{-1}) and TRB (8.9 ± 1.8 g kg^{-1}).

Considering the sampling sites' ranges of the above-mentioned soil fertility variables, the Marl site shows the most and the Gneiss site the least ideal conditions. The Marl site's pH values are within a range, where essential plant micronutrients and phosphorus are plant available (Barrow et al., 2020; Blume et al., 2016). The given pH range together with the Marl site's bulk soil C:N values support microbial processing and hence the decomposition of OM to nutrients and energy for plant and microbial growth (Brust, 2019; Barrow et al., 2020; Currie, 2003; Myrold and Bottomley, 2008). The Marl site also has the overall highest CEC and TRB values which support nutrient retention in the soil (Blume et al., 2016).

https://doi.org/10.5194/egusphere-2025-2006
Preprint. Discussion started: 14 May 2025

3.1.2 Soil mineralogy

Average Fe_{DCB}/Fe_{tot} ratios are highest at the Marl and Gneiss sites (0.72 ± 0.22 vs. 0.68 ± 0.18, respectively) and smallest at the Flysch site (0.38 ± 0.08) (Table 4). Average sand content is highest (58.9 ± 7.1 %) and clay content is lowest (3.8 ± 0.7 %) at the Gneiss site. The largest average clay content is at the Marl site (13.7 ± 5.8 %). The average sum of pedogenic oxides ΣPed ox_{PP+AO}) is highest at the Gneiss and Greenschist sites (18.0 ± 1.6 vs. 18.4 ± 1.6 g kg^{-1}, respectively) and lowest at the Flysch site (8.7 ± 1.7 g kg^{-1}).

Considering the sampling sites' ranges of the above-mentioned soil mineralogy variables, the Marl and Gneiss sites show the most ideal conditions for SOC stabilization by having the highest respective clay content and pedogenic oxide concentrations. With the second-highest overall pedogenic oxide concentrations of all sites, Greenschist also possesses good conditions for potential SOC stabilization. The Flysch site has the overall least ideal conditions by possessing the lowest concentrations of pedogenic oxides and simultaneously having a relatively low clay content.

3.2 Above- and belowground biomass organic carbon stocks and soil organic carbon stocks

Across all sites, the significantly largest ABM OC stock can be found at the Gneiss site, amounting to 754 ± 144 g C m^{-2} (Fig. 3 (a)). Of which an approximate 80 % consists of woody plant material. The Dolomite and Marl sites show the lowest aboveground biomass OC stocks (147 ± 12 and 140 ± 31 g C m^{-2} respectively), while not varying significantly from that of the Flysch and Greenschist sites. The highest belowground biomass OC stocks can be found at the Flysch and Marl sites (91 ± 10 and 97.3 ± 24 g C m^{-2} respectively), which are approximately three times larger than those of the other sites. These two sites also show a more constrained average above- to belowground biomass OC stock ratios of ∼1.6–2.5, compared to the other sites with ratios of 4 up until 22 for the Gneiss site.

The largest whole profile SOC stocks can be found on the Gneiss site, closely followed by those of the Marl site, that showed no statistically significant difference (23.2 ± 1.9 and 21.3 ± 4.3 kg C m^{-2} respectively) (Fig. 3 (b)). The smallest whole profile SOC stocks can be found on the Flysch and Dolomite sites (8.1 ± 1.2 and 9.5 ± 1.5 kg C m^{-2} respectively), which are significantly smaller than the stocks of the other three sites. Across all sites, the largest horizon-specific stocks are contained within the Bw horizons, that contribute an approximate 74–87 % to whole profile SOC stocks. The smallest horizon specific SOC stocks are those of the Cw horizons. These findings are linked to the SOC stock calculation methodology, which depends on the thickness of individual soil horizons and their OC contents (Sect. 2.3.7). Because the Bw horizons were the thickest on average, they harbor the overall largest SOC stocks. Despite containing lower SOC concentrations than the sampled Oh and Ah horizons (Fig. 2, Sect. 2.1).

https://doi.org/10.5194/egusphere-2025-2006
Preprint. Discussion started: 14 May 2025

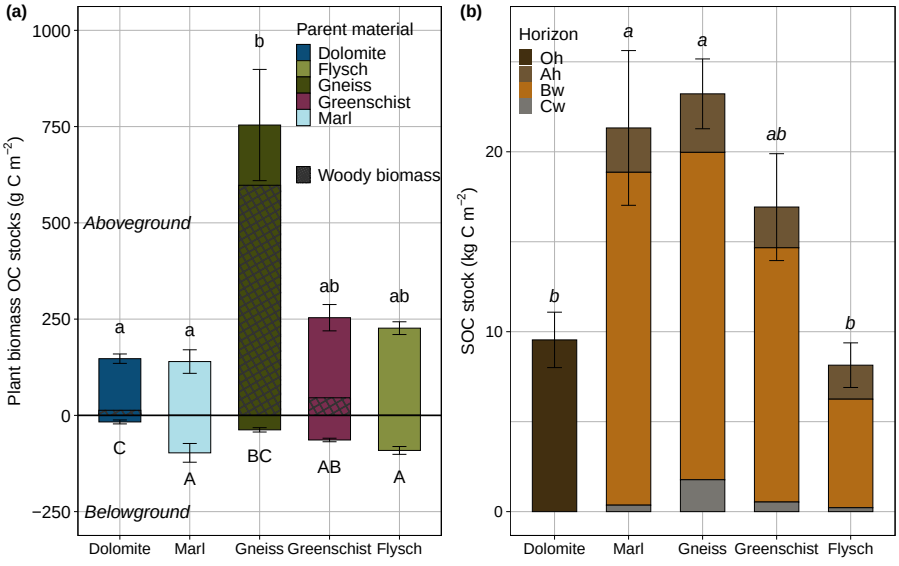

Figure 3. (a) Average total above- and belowground plant biomass OC stocks (g C m^{-2}) ± standard errors across all sites. Aboveground biomass values are depicted as > 0 and belowground as < 0 for illustrative purposes. The presence and magnitude of woody vs. non-woody aboveground plant biomass is represented by the extent of the black crosshatch pattern. **(b)** Average total SOC stocks (kg C m^{-2}) ± standard errors, split into individual horizon SOC stocks, across all sites. Same respective lowercase, or uppercase letters denote total above-/belowground plant OC or whole profile SOC stocks, that are not statistically significant from one another.

3.3 $F^{14}C$ and the relative contribution of soil fractions to bulk soil organic carbon

Across all sites there is a depth/horizon-dependent decrease in $F^{14}C$ values (Fig. 4 (a)). The overall smallest $F^{14}C$ values are found at the Marl and Gneiss sites. Hereby, the Marl site displays a smaller value for the Cw horizon than the Gneiss site (0.77 vs. 0.82 respectively) but a slightly higher value for the Bw horizon compared to the Gneiss site (0.97 vs. 0.95 respectively). The greatest overall $F^{14}C$ values for all soil horizons can be found for the Greenschist site. Ranging from 1.06–0.88 from the Ah to the Cw horizon. All sites' Ah horizons are modern in terms of $F^{14}C$, with values > 1. However, Marl site's Ah horizon seems to include slightly greater amounts of more persistent C, leading to a slightly smaller $F^{14}C$ value of 1.04, compared to the value of 1.06 for the other sites. The only other horizon that is deemed modern is the Bw horizon of the Greenschist site.

The importance of a fraction's relative contribution to bulk SOC (%) varies within each site's soil horizons and across all sites (Fig. 4 (b)). A first overarching trend across all sites can be found for the relative contribution of POM to bulk SOC (%), which increasing with increasing bulk SOC (%). The POM fraction's relative contribution to bulk SOC varies the most of all fractions and ranges between 1–73 % (Fig. 4 (b), POM). The s+c fraction's contribution to bulk SOC decreases rather linearly with increasing bulk SOC. It therefore displays a trend opposite to that of the POM fraction. The s+c fraction's overall contribution ranges from 3–44 % to bulk SOC (%) (Fig. 4 (b), s+c). In contrast, the relative contribution of the MA fraction to

https://doi.org/10.5194/egusphere-2025-2006
Preprint. Discussion started: 14 May 2025

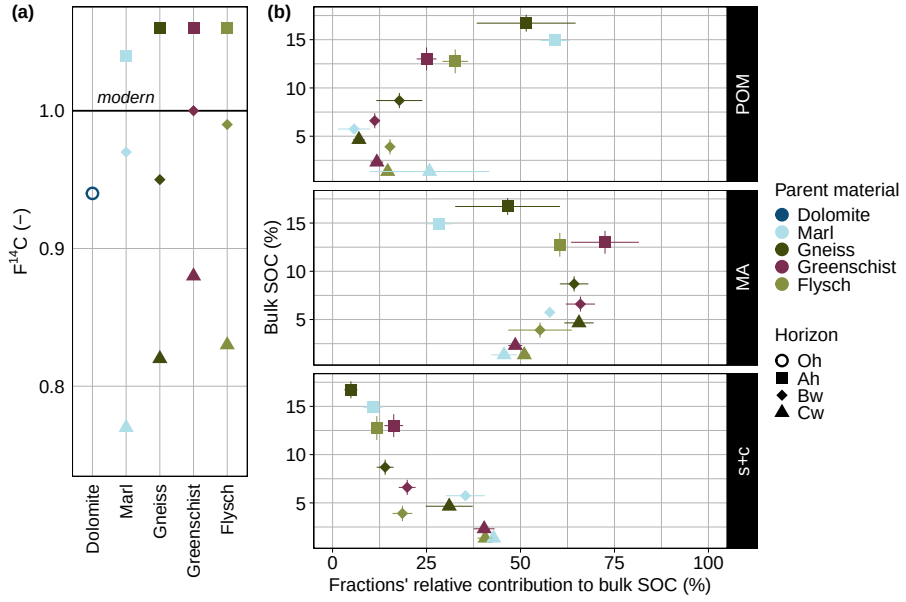

Figure 4. (a) $F^{14}C$ of all soil horizons and sites. Note that all values > 1 are defined as modern. **(b)** Average bulk SOC (%) ± standard errors vs. the average relative contributions of the three examined fractions POM, MA and s+c to bulk SOC (%) ± standard errors are shown across all sites and their individual horizons. Observations from the Dolomite site were excluded from this figure as its Oh horizon is organic and showed signs of POM contamination in the MA fraction.

bulk SOC does not show a clear pattern with varying bulk SOC content. This fraction's relative contribution to bulk SOC is > 25 % across all soil horizons of all sites, with most values lying within 45–75 % (Fig. 4, MA).

3.4 Soil organic carbon model predictions with soil fertility versus soil mineralogical parameters

Both the soil fertility and the soil mineralogy model's predictions of bulk SOC content (%) aligned well with the observed SOC values (Fig. 5 (a) and (c)). The soil fertility model slightly outperforms the soil mineralogy model with an R^2 of 0.91 and an RMSE of 2.02, compared to an R^2 of 0.84 and an RMSE of 2.52. Bio-P has the highest relative importance for the soil fertility model, with a value of 20 % and has a significant positive correlation coefficient of 0.86 with bulk SOC (Fig. B1). Clay is among the most important predictor variables for both models, with a relative variable importance of 17.7 and 24.2 % for the soil fertility and soil mineralogy model, respectively (Fig. 5 (b) and (d)). Clay shows a significant negative correlation coefficient of -0.77 with SOC (Fig. B1, Fig. B2). The soil fertility model's predictor variables are all significantly, positively correlated with SOC content except for clay, exchangeable K (K_{ex}) and pH, which are negatively correlated. The soil mineralogy models' organically-complexed Fe_{PP}, Al_{PP} and Mn_{PP} oxides are all positively correlated with SOC content, while the poorly crystalline Fe_{AO}, Al_{AO} and Mn_{AO} oxides correlate negatively with SOC with varying degrees of significance (Fig. B2).

https://doi.org/10.5194/egusphere-2025-2006
Preprint. Discussion started: 14 May 2025

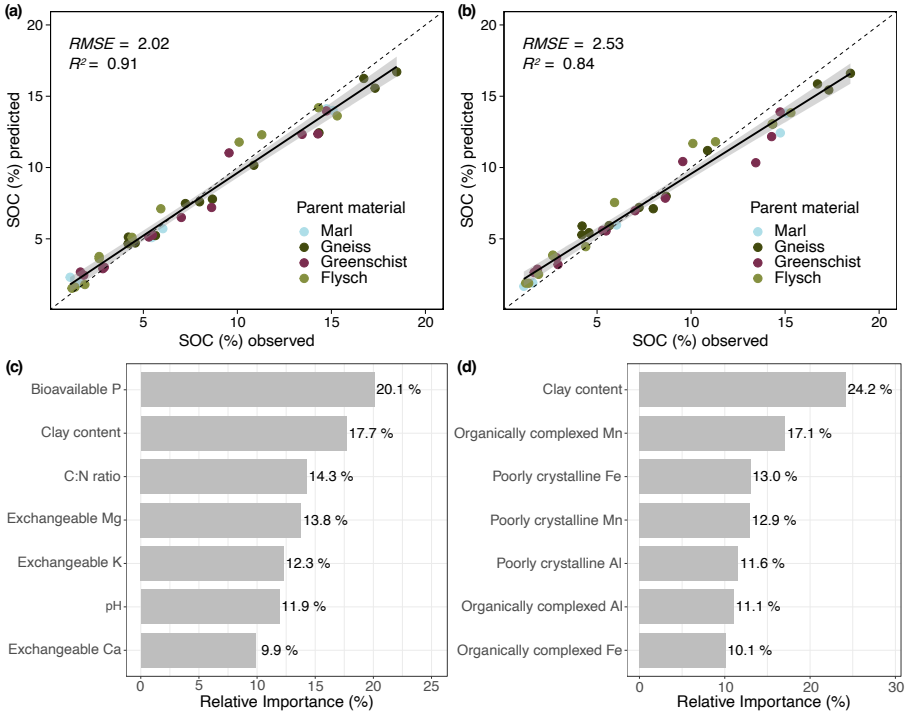

Figure 5. (a) Predicted bulk SOC (%) values vs. measured/observed bulk SOC (%) values of the soil fertility model. **(b)** Predicted bulk SOC (%) values vs. measured/observed bulk SOC (%) values of the soil mineralogy model. **(c)** Relative importance (%) of the model predictor variables included in the soil mineralogy model. **(d)** Relative importance (%) of the model predictor variables included in the soil fertility model.

4 Discussion

4.1 Largest biomass organic carbon stocks found on low fertility soil

Against the posited hypothesis that nutrient-rich soils with a high mineral weatherability, such as those of the Marl or Greenschist sites, would display the largest plant biomass OC stocks, the highest total plant biomass OC stocks were found at the Gneiss site (Fig. 3 (a)). These high stocks are mostly attributable to the Gneiss site's ABM stocks which contribute approximately 95 ± 25 % to total plant biomass OC stocks. The acidic pH at this site supports the growth of shrubs from the Vaccinium genus (Chen et al., 2019), which coincide with a very high percentage of woody biomass and wide C:N ratios (Fig. 3 (a), Table 4). The greater aboveground plant biomass of this Vaccinium-dominated site, and its slightly elevated composite plant biomass C concentration (46.3 vs. 43.9–44.1 % compared to all sites except Greenschist), result in the observed large ABM OC stocks. Despite the Gneiss site having among the lowest measured CEC_{eff} and TRB (Table 4) we infer that the Vaccinium shrubs are able to support their relatively large ABM through N fixation and facilitated uptake of P by mycorrhizal roots (Jiang et al., 2024; Vohník and Réblová, 2023; Daghino et al., 2022; Püschel et al., 2021). Recently, Zhao et al. (2023) also showed that shrub

https://doi.org/10.5194/egusphere-2025-2006
Preprint. Discussion started: 14 May 2025

encroachment in alpine grasslands of the Tibetan Plateau lead to increased aboveground biomass compared to non-encroached sites. Despite its large ABM, the Gneiss site has significantly smaller BBM OC stocks than those of the Marl, Flysch and also Greenschist sites (Fig. 3 (a)). The Dolomite site also exhibits low plant biomass OC stocks, which is typical for the little developed, nutrient-poor soil (Pignatti and Pignatti, 2014). In contrast to ABM OC stocks, the differences in BBM OC stocks appear to more closely follow differences in CEC_{eff}, TRB and clay, which all contribute to soil fertility. The differences in these BBM OC stocks are also reflected by the relative rooting depth differences within the different sites' soil profiles (Fig. 2). Overall, the above- and belowground biomass of all sites measured in the context of this study (240–2440 g m^{-2} and 14–320 g m^{-2}, for above- and belowground biomass, respectively) lie within a similar range of above- and belowground biomass reported for a medium alpine altitudes under closed alpine vegetation (100–1500 g m^{-2} and ca. 500–700 g m^{-2}, for above- and belowground biomass, respectively) (Leifeld et al., 2009; Hitz et al., 2001).

In summary, the importance of soil fertility variables such as CEC_{eff}, TRB and clay for biomass production seem to have a more pronounced effect on BBM OC stocks than ABM OC stocks. Our data shows that ABM OC stocks can become large despite soils not being nutrient rich or displaying high CEC_{eff} values, yet displaying properties that favour the growth of specific, site-adapted plant functional types.

4.2 Magnitude of biomass organic carbon stocks not necessarily linked to magnitude of soil organic carbon stocks - importance of soil stabilization mechanisms

The highest overall SOC stocks were found at the Gneiss and Marl sites (Fig. 3 (b)). Since the Gneiss site harbours the highest plant biomass OC stocks, our hypothesis that high biomass OC stocks may lead to, or coincide with, the largest SOC stocks therefore seems true at first glance. Increased SOC stocks under shrub-encroached, alpine grasslands were also found on the Tibetan Plateau (Zhao et al., 2023). This shrub-induced increase in SOC stocks is presumably linked to the high sand content found at the Gneiss site. A meta-analysis of worldwide shrub-encroached grasslands showed that resulting SOC content changes were soil texture dependent, with decreases in silty and clay soils and increases in sandy soils (Li et al., 2016). However, the Marl site possesses a much smaller total plant biomass OC stock yet bears comparable SOC stocks. Thus, overall magnitude of total plant biomass does not necessarily determine or coincide with SOC accrual. Therefore the potential of soil stabilization mechanisms must be considered additionally, as we hypothesized. This becomes all the more apparent considering the Flysch site which has a greater ABM and comparable BBM OC stocks to the Marl site. Yet, the Flysch site's SOC stock is only approximately one third the size of the Marl and Gneiss site's SOC stocks. These findings contradict those of Nie et al. (2023), that found a significant correlation, while moderate in strength, between ABM and BBM on SOC stocks across alpine meadows of the Tibetan Plateau. The Dolomite site's small SOC stocks are likely caused by the absence of mineral horizon formation, limiting the accumulation of greater SOC stocks at this site. The lack of mineral horizons are the result of the high solubility/weatherability of the Dolomite site's parent material (Brady and Weil, 2008). Nevertheless, the Dolomite site's thick Oh horizon still holds SOC stocks comparable to whole profile SOC stocks of the Flysch site. Despite the Flysch site having developed a deeper soil profile including mineral horizons (Fig. 2, Fig. 3 (b)). On the whole, the SOC stocks of all sites we

https://doi.org/10.5194/egusphere-2025-2006
Preprint. Discussion started: 14 May 2025

report here (8–23 kg C m^{-2}) lie within a similar range of SOC stocks reported for medium alpine altitudes under closed alpine vegetation (4–22 kg C m^{-2}) (Webber and May, 1977; Canedoli et al., 2020; Leifeld et al., 2009)).

Our second hypothesis stated that pedogenic oxides and not the amount of clay would ultimately coincide with greater SOC stocks. Supportive of this hypothesis is the positive relationship between Fe_{PP+AO} pedogenic oxide concentrations and horizon-dependent SOC stocks, with the highest Fe_{PP+AO} pedogenic oxide concentrations coinciding with the highest SOC stocks in the Bw horizons (data not shown). In comparison, the relationship between Al_{PP+AO} and Mn_{PP+AO} pedogenic oxides and SOC stocks (data not shown) and SOC content (Fig. B2) is less evident. Past work has reported varying importance of Al_{PP+AO} compared to Fe_{PP+AO}. With some studies reporting a stronger relationship between Al_{AO} and SOC than Fe_{AO} and SOC (Hall and Thompson, 2022; Percival et al., 2000) and other work demonstrating the relevance of both Al_{AO} and Fe_{AO} to SOC stabilization in cold and wet ecosystem (Yu et al., 2021). Nevertheless, across all sites, the highest sum of Fe_{PP+AO} and Al_{PP+AO} pedogenic oxide concentrations are located at the Gneiss and Greenschist sites, as a result of their mafic parent materials. The co-occurence of high Fe_{PP+AO} and Al_{PP+AO} pedogenic oxide concentrations and the largest SOC stocks at the Gneiss site, underline the importance of pedogenic oxides in SOC stabilization there, especially since the Gneiss site has a very low clay content (Table 4. In contrast, the Marl site, which holds similarly large SOC stocks as the Gneiss site, has the lowest Fe_{PP+AO} concentrations and smaller Al_{PP+AO} concentrations. Concomitantly, the Marl site has the highest clay content of all sites and may thus be of higher importance at this site for SOC stabilization through complexation and adsorption on reactive clay surfaces but also by promoting the production of aggregates (Six et al., 2002; Lützow et al., 2006). The larger importance of clay-mediated SOC stabilization processes at the Marl site is supported by a greater contribution of this site's s+c fraction C to bulk SOC in the Bw horizon compared to that of the other sites (Fig. 4, (b)).

In summary, the formation of organo-metal complexes and association of OC with poorly crystalline Fe and Al oxides and short-range order (SRO) minerals pose an important mechanism contributing to overall SOC stocks. Especially, in soils developed on siliceous and mafic rocks, rich in Fe and Al, such as at the Gneiss or Greenschist sites. In soils with higher clay content and lower concentrations of Fe and Al pedogenic oxides, such as the Marl site, clay still contributes significantly to SOC stabilization.

4.3 SOC persistence not explicable by soil fraction differences

The Marl and Gneiss sites hold the most persistent SOC of all sites in their subsoil horizons (Bw, Cw), with the smallest horizon-specific $F^{14}C$ values, excluding the Dolomite site's single observation (Fig. 4 (a)). The soils of the Gneiss and Marl sites have undergone stronger weathering, in terms of Fe_{DCB}/Fe_{tot} (Fig. 2, Table 4). Despite this, these sites' soils do not have clear, greater contributions of MA or s+c to bulk SOC in comparison to all other sites, except for the Marl site's Bw horizon. Therefore our general hypothesis, that soils with more persistent SOC would have developed increased mineral-related stabilization mechanisms, compared to soils with less persistent SOC, must be rejected for most sites. The Marl site's Bw horizon marks a exception with a $\geq$ 1.5 time higher contribution of s+c to bulk SOC (%) compared to all other sites' Bw horizons,

https://doi.org/10.5194/egusphere-2025-2006
Preprint. Discussion started: 14 May 2025

which show a relatively similar relative contribution of s+c to bulk SOC. With regard to the relative contribution of MA to bulk SOC, however, the Marl site's Bw horizon shows values similar to those of the other sites (Fig. 4 (b). The higher SOC persistence of the Gneiss and Marl sites' subsoils, taken together with the importance of MA and s+c fraction's contribution to bulk SOC in these sites' Bw horizons, suggest that the majority of these sites' SOC stocks are rather stabilization than input-driven. In comparison, the Greenschist site, which has the largest $F^{14}C$ values across all horizons of all sites including modern values for its Bw horizon, seems to be more input-driven with a potentially higher turnover of OC. A study on a 2200 km grassland transect on the Tibetan Plateau also found that topsoil (0–10 cm) $\Delta^{14}C$ values were plant OC input controlled compared to subsoil (30–50 cm) $\Delta^{14}C$ values, which depended on mineral stabilization mechanisms (Chen et al., 2021).

In contrast to their subsoils, the modern Ah horizons of the Gneiss and Marl sites show a much larger contribution of POM to the Ah horizons' bulk SOC (> 50 %). The absolute and relative importance of POM to the Ah horizon of the Gneiss site is presumably linked to the large, woody-biomass-dominated ABM OC stock, and thus potential input into the soil (Fig. 4, Table A1). The wide C:N ratio of the Gneiss site's ABM may also lead to reduced decomposition, and thus accumulation, of POM in the soil (Liang et al., 2017). At the Marl site the significance of POM to bulk SOC may result from its large production of belowground biomass OC (Fig. 3 (a)). For all other horizons no clear differences can be seen regarding relative fraction contributions to bulk SOC across the sites. The only clear trend in relative fraction contributions to bulk SOC is visible with increasing soil depth, where the contribution of s+c increases while that of POM diminishes. This finding further supports the initial hypothesis that clay as a particle size alone is less important a contributing factor to SOC stocks across all sites, except the Marl site.

In general, the MA fraction represents the most important SOC stabilization fraction, contributing > 25 % to bulk SOC (%), across all soil horizons of all sites (Fig. 4, MA). The importance of the MA formation for SOC stabilization is also reflected by it contributing the most, out of all analyzed fractions, to bulk SOC within Bw horizons. The overall thickest horizons, with the largest relative contribution to whole profile SOC stocks, except for the Dolomite site (Fig. 2, Fig. 3 (b)). A large importance of MA to bulk SOC was also found in Chilean grassland topsoils under cold climates with high bulk SOC contents (Wasner et al., 2024). The larger contribution of the MA fraction to bulk SOC cannot be explained by a significantly larger presence of fraction-specific Fe or Al concentrations, as the elemental analysis revealed no clear differences between the MA and s+c fractions (data not shown).

In summary, though the most weathered soils of the Gneiss and Marl sites display the most persistent bulk OC values, they did not show a larger contribution of mineral-stabilized C to bulk SOC, compared to all other sites. These two sites also correspond to the largest SOC stocks, that appear to be rather stabilization than input-driven. Further, across all sites and horizons a large contribution of MA was found to contribute to bulk SOC, demonstrating the importance of aggregation processes for SOC stabilization in alpine soils developed on different parent materials.

https://doi.org/10.5194/egusphere-2025-2006
Preprint. Discussion started: 14 May 2025

4.4 SOC content predicted equally well with soil fertility and soil mineralogical variables

Both SOC prediction models performed similarly well, despite portraying two different sets of drivers (Fig. 5). We interpret this finding as follows- that both soil fertility as well as soil mineralogical parameters are equally important in determining SOC content and that both sets of parameters can ultimately contribute to SOC accrual. In both models clay appears as one of the most important predictor variables of SOC content, despite recent work reporting other variables as better predictors of SOC content. Such as exchangeable Ca in water-limited soils and Fe and Al oxy(hydr-)oxides in wet, acidic soils (Rasmussen et al., 2018; von Fromm et al., 2021). We assume that on the site-level one model may outperform the other, depending on which set of parameters ultimately matter more at a specific site. For example, we assume that the soil fertility model could more accurately predict SOC of sites that show higher values of soil fertility-enhancing parameters, e.g. TRB, bio-P, clay and simultaneously possess smaller values of properties that would enable a greater mineralogical stabilization potential for SOC, e.g. pedogenic oxides. This may be the case for the Flysch site's soil (Fig. 2, Table 4, Table A1). We therefore also assume that the soil mineralogy model could more accurately predict SOC of more strongly weathered soils, such as those of the Marl or Gneiss site, that have developed properties as mentioned above, enabling greater mineralogical stabilization potentials. However, due to the limited number of observations, we cannot confirm which of the two models leads to more accurate SOC predictions for each respective site. To assess the validity of our aforementioned assumptions, a larger number of observations would be required than those provided in this study.

5 Conclusions

This study explored how parent material geochemistry affects soil properties and, in turn, influences plant biomass OC and SOC accumulation, through differences in resulting soil stabilization potentials and soil fertility in European alpine grasslands. Contrary to expectations, neither above- nor belowground plant biomass OC stocks were primary elements shaping whole profile SOC stocks. Instead, our data shows that more weathered soils developed deeper profiles and accumulated substantially greater SOC stocks, largely due to enhanced stabilization potential. Hereby, sites rich in Fe and Al pedogenic oxides facilitated increased organo-metal complexation and occlusion of SOC by microaggregates. While clay had a relatively minor role in most soils, it was a notable contributor to SOC stock accrual at the site with the highest clay content and most persistent SOC. Across all study sites, microaggregates emerged as the most important universal SOC-stabilizing phase, contributing ≥ 50 % to bulk SOC in most soils. Thus, we propose that future research should investigate how pH, oxy(hydr-)oxides and plant biomass inputs influence microaggregate formation, composition and stability across alpine soils of varying weathering stages. Finally, by applying a random forest model, we demonstrated that SOC content in the examined alpine soils could be predicted equally well by a set of soil fertility or mineralogical variables- underscoring the dual importance of both soil fertility and mineralogy in determining SOC.

https://doi.org/10.5194/egusphere-2025-2006
Preprint. Discussion started: 14 May 2025

Code and data availability. Datasets used for this publication are available on Zenodo (https://doi.org/10.5281/zenodo.15282598, Maier et al., (pre publication version) as are the R code scripts (https://doi.org/10.5281/zenodo.15282213, Maier et al., (pre publication version).

Appendix A

https://doi.org/10.5194/egusphere-2025-2006
Preprint. Discussion started: 14 May 2025

Table 4. Average ± standard errors of C:N (-), pH (-), bio-P (mg kg^{-1}), CEC_{eff} (cmol kg^{-1}), TRB (g kg^{-1}), the sum of Al, Fe and Mn PP- and AO-extractable pedogenic oxides (ΣPed ox_{PP+AO}) (g kg^{-1}), Fe_{tot}/Fe_{DCB} (-), sand (%) and clay (%) split into the following samples: aboveground biomass (ABM), belowground biomass (BBM) and individual soil horizons Ah, Bw, Cw.

Parent material	Sample	C:N	pH	Bio-P	CEC_{eff}	TRB	ΣPed ox_{PP+AO}	Fe_{DCB}/Fe_{tot}	Sand	Clay
Dolomite	ABM	31.4 ± 1.8	-	-	-	-	-	-	-	-
	BBM	39.6 ± 3.3	-	-	-	-	-	-	-	-
	Oh	12.8 ± 1.4	5.1 ± 0.2	54.4 ± 12.3	46.1 ± 3.3	19.7 ± 1.5	11.1 ± 1.4	0.79 ± 0.02	66.8 ± 1.4	1.3 ± 0.2
Marl	ABM	27.8 ± 5.4	-	-	-	-	-	-	-	-
	BBM	33.8 ± 3.7	-	-	-	-	-	-	-	-
	Ah	12.5 ± 0.6	5.3 ± 0.4	34 ± 3.5	32.9 ± 2.9	15.3 ± 3.8	11.1 ± 3.3	0.82 ± 0.21	73.8 ± 5.3	3.1 ± 0.9
	Bw	10.0 ± 0.5	4.8 ± 0.6	2.3 ± 0.4	17.9 ± 0.3	16.9 ± 0.5	14.6 ± 4.0	0.70 ± 0.01	28.2 ± 12.1	15.7 ± 5.7
	Cw	11.0 ± 1.9	6.6 ± 0.2	1.7 ± 1.4	24.1 ± 0.3	67.8 ± 46.0	7.6 ± 0.6	0.65 ± 0.06	11.1 ± 0.9	32.2 ± 0.0
Gneiss	ABM	40.7 ± 2.0	-	-	-	-	-	-	-	-
	BBM	84.4 ± 12.8	-	-	-	-	-	-	-	-
	Ah	17.5 ± 0.9	3.7 ± 0.1	33.8 ± 11.5	15.6 ± 0.9	7.3 ± 1.2	12.3 ± 1.2	0.81 ± 0.18	74.7 ± 6.1	1.4 ± 0.4
	Bw	15.8 ± 0.9	3.7 ± 0.1	3.2 ± 0.3	8.9 ± 0.5	8.6 ± 0.9	20.9 ± 0.7	0.67 ± 0.03	44.8 ± 2.7	4.9 ± 0.5
	Cw	15.1 ± 0.8	4.0 ± 0.0	0.9 ± 0.2	5.1 ± 0.7	10.7 ± 0.9	21.9 ± 0.7	0.56 ± 0.02	57.1 ± 2.5	5 ± 0.3
Greenschist	ABM	60.8 ± 4.0	-	-	-	-	-	-	-	-
	BBM	75.1 ± 11.6	-	-	-	-	-	-	-	-
	Ah	13.5 ± 0.1	5.0 ± 0.2	22.4 ± 3.3	29.6 ± 0.4	40.3 ± 3.7	15.8 ± 0.9	0.56 ± 0.02	55.7 ± 3.2	4.6 ± 0.5
	Bw	11.2 ± 0.2	4.7 ± 0.2	3.8 ± 0.5	17.8 ± 0.8	47.4 ± 4.8	20.5 ± 0.8	0.55 ± 0.03	22.1 ± 3.0	12.1 ± 1.1
	Cw	11.9 ± 0.1	5.0 ± 0.1	0.6 ± 0.1	15.1 ± 0.9	82.3 ± 5.7	17.7 ± 1.1	0.35 ± 0.03	19.8 ± 2.0	12.9 ± 0.6
Flysch	ABM	25.9 ± 1.0	-	-	-	-	-	-	-	-
	BBM	30.5 ± 2.1	-	-	-	-	-	-	-	-
	Ah	12.0 ± 0.4	5.1 ± 0.2	50.4 ± 6.6	22.7 ± 3.2	15.4 ± 1.7	7.5 ± 0.8	0.38 ± 0.04	62.5 ± 3.4	2.4 ± 0.4
	Bw	9.5 ± 0.6	4.6 ± 0.3	6.1 ± 1.8	8.8 ± 1.2	14.3 ± 1.6	9.7 ± 1.2	0.39 ± 0.06	32.5 ± 3.5	6.0 ± 0.5
	Cw	7.5 ± 0.1	5.1 ± 0.4	1.1 ± 0.2	6.9 ± 0.5	15.5 ± 1.8	8.8 ± 1.0	0.37 ± 0.04	24.9 ± 1.9	7.1 ± 0.5

https://doi.org/10.5194/egusphere-2025-2006
Preprint. Discussion started: 14 May 2025

Table A1. Overview of the results from the soil fractionation procedure. All results are reported as averaged values ± the standard deviation. Fractionation mass loss shows how much sample material was lost during the fractionation procedure relative to the amount of initially weighed-in bulk soil, where positive values indicate a net mass loss and negative values indicate a supposed mass increase post-fractionation. The fraction percentages of POM, MA, and s + c are related to the total soil present after soil fractionation.

Parent material	**Horizon**	**Fractionation mass loss (%)**	**POM (%)**	**MA (%)**	**s + c (%)**
Dolomite	Oh	6.9 ± 1.4	32.6 ± 11.6	54.0 ± 11.6	13.5 ± 0.7
Marl	Ah	4.6 ± 0.5	38.9 ± 27.4	45.3 ± 18.7	15.8 ± 8.6
	Bw	2.5 ± 1.0	30.2 ± 9.1	41.2 ± 11.5	28.5 ± 4.1
	Cw	0.8 ± 0.9	17.1 ± 3.9	29.8 ± 16.1	53.2 ± 19.6
Gneiss	Ah	3.0 ± 1.8	57.5 ± 18.4	37.6 ± 15.8	4.9 ± 9.8
	Bw	2.2 ± 0.7	37.3 ± 7.8	52.3 ± 5.0	10.4 ± 7.3
	Cw	2.8 ± 1.0	38.6 ± 0.8	46.9 ± 2.6	14.5 ± 8.9
Greenschist	Ah	4.2 ± 2.3	19.6 ± 1.1	57.6 ± 4.8	22.8 ± 3.7
	Bw	2.3 ± 0.7	14.2 ± 4.5	61.3 ± 5.0	24.5 ± 3.9
	Cw	1.1 ± 0.9	30.3 ± 4.3	40.7 ± 2.4	29.0 ± 2.7
Flysch	Ah	2.2 ± 1.4	32.9 ± 3.1	49.4 ± 3.0	17.8 ± 3.5
	Bw	-8.2 ± 15.9	32.7 ± 8.9	44.6 ± 7.7	22.7 ± 8.2
	Cw	-0.1 ± 0.5	35.2 ± 1.6	37.1 ± 5.5	27.7 ± 3.9

https://doi.org/10.5194/egusphere-2025-2006
Preprint. Discussion started: 14 May 2025

Appendix B

Table B1. Overview of the linear regression, least-angle regression, elastic net regression and random forest model performance metrics (R^2, RMSE). All results are reported as averaged values of 100 model runs.

Model	**Soil fertility variables**		**Soil mineralogy variables**	
	R^2	RMSE	R^2	RMSE
Linear regression	0.90	2.05	0.72	2.96
Least-angle regression	0.88	2.09	0.70	3.06
Elastic net regression	0.89	2.02	0.70	3.04
Random forest	0.89	2.07	0.81	2.56

https://doi.org/10.5194/egusphere-2025-2006
Preprint. Discussion started: 14 May 2025

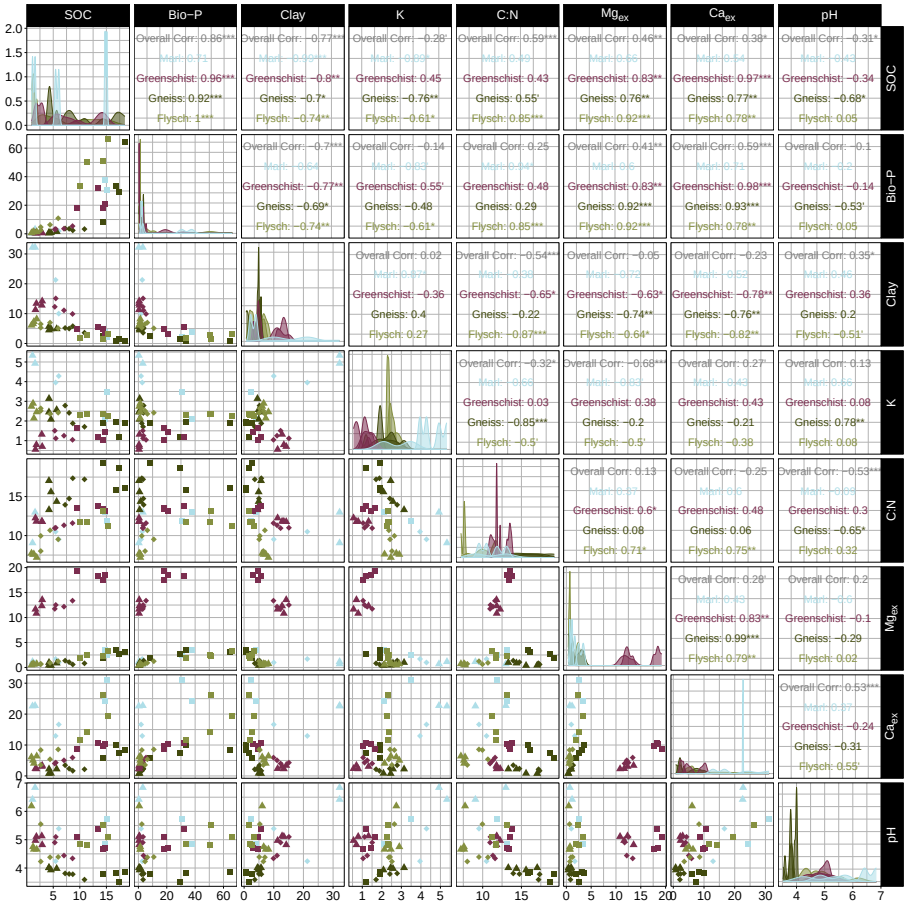

Figure B1. In the left half of the matrix, scatterplots show the relationship between all soil fertility model predictor variables and SOC. Observations are shown considering individual parent materials and horizons, corresponding to different respective colours and shapes. Where Ah are squares, Bw diamonds and Cw triangles. Diagonally, density plots show observation frequencies for respective predictor variables are displayed and split into individual parent materials, according to different allocated colours. In the right half of the matrix, spearman correlations coefficients for all soil fertility model predictor variables and SOC, considering all observations (Overall Corr) and individual parent materials, corresponding to different respective colours. Note that "***", "**", "*", "'", " " indicate p-values of < 0.001, < 0.01, < 0.05, < 0.1 and ≥ 0.1 that are allocated to the correlation coefficients. Dolomite observations are excluded as its observations were not considered in the SOC model predictions.

https://doi.org/10.5194/egusphere-2025-2006
Preprint. Discussion started: 14 May 2025

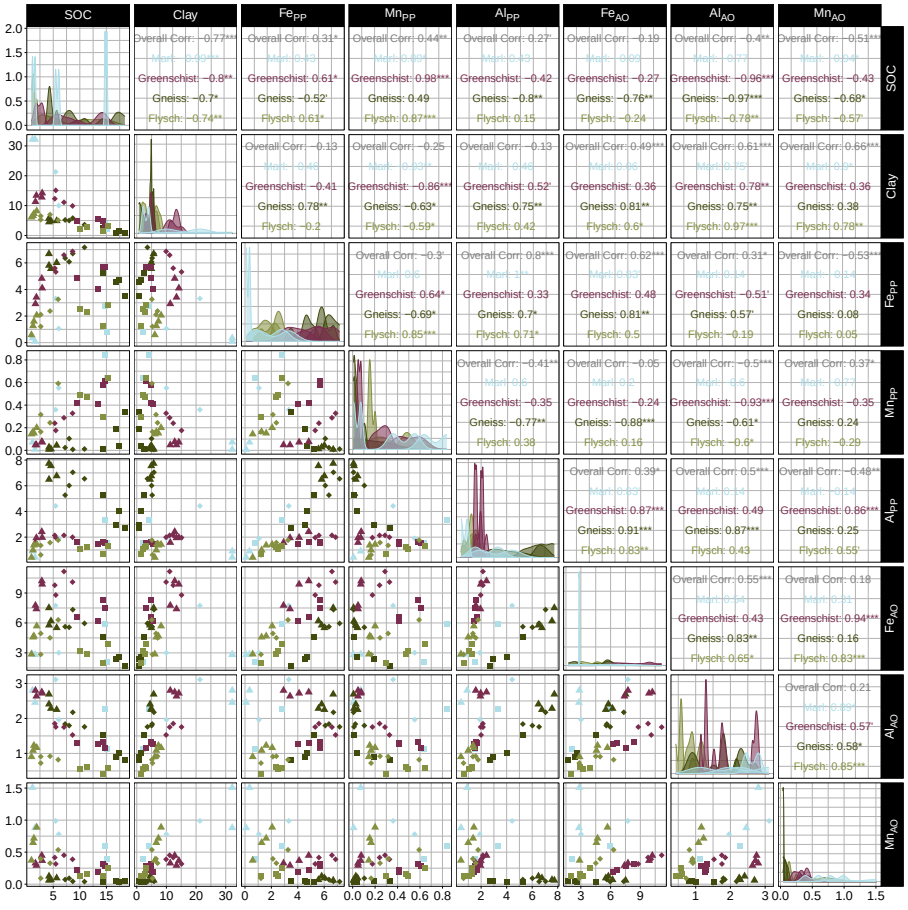

Figure B2. In the left half of the matrix, scatterplots show the relationship between all soil mineralogy model predictor variables and SOC. Observations are shown considering individual parent materials and horizons, corresponding to different respective colours and shapes. Where Ah are squares, Bw diamonds and Cw triangles. Diagonally, density plots show observation frequencies for respective predictor variables are displayed and split into individual parent materials, according to different allocated colours. In the right half of the matrix, spearman correlations coefficients for all soil mineralogy model predictor variables and SOC, considering all observations (Overall Corr) and individual parent materials, corresponding to different respective colours. Note that "***", "**", "*", "'", " " indicate p-values of < 0.001, < 0.01, < 0.05, < 0.1 and ≥ 0.1 that are allocated to the correlation coefficients. Dolomite observations are excluded as its observations were not considered in the SOC model predictions.

https://doi.org/10.5194/egusphere-2025-2006
Preprint. Discussion started: 14 May 2025

Author contributions. The conceptualization of the study for this paper was done by MG and SD and MG. Development of the methodology was done by SD and MG. Samples were collected and investigated by MM and MG. Data curation and validation was done by MM and AM. All formal analyses and visualizations were performed by AM except for the statistical model, which was performed by MM. AM wrote the final draft, based loosely off an earlier version by MM. All authors contributed to the editing and the revision of the paper.

Competing interests. The authors declare no competing interests.

Acknowledgements. The authors would like to thank Chigusa Keller, Loïc Imsand, Daniel Abgottspon, Anna Stegmann and Julia Mayrock for assistance during sample collection. Furthermore the authors would like to thank Julia Franzen for assisting in sample preparation and Jessica Carilli for conducting some of the laboratory analyses. The authors acknowledge the use of artificial intelligence (AI) in revising small segments of the R code for the data analysis pipeline.

https://doi.org/10.5194/egusphere-2025-2006
Preprint. Discussion started: 14 May 2025

References

Anderson, K., Fawcett, D., Cugulliere, A., Benford, S., Jones, D., and Leng, R.: Vegetation expansion in the subnival Hindu Kush Himalaya, Glob. Change Biol., 26, 1608–1625, https://doi.org/10.1111/gcb.14919, 2020.

Augusto, L., Achat, D. L., Jonard, M., Vidal, D., and Ringeval, B.: Soil parent material- A major driver of plant nutrient limitations in terrestrial ecosystems, Glob. Change Biol., 23, 3808–3824, https://doi.org/10.1111/gcb.13691, 2017.

Baldock, J. and Skjemstad, J.: Role of the soil matrix and minerals in protecting natural organic materials against biological attack, Org. Geochem., 31, 697–710, https://doi.org/10.1016/S0146-6380(00)00049-8, 2000.

Barrow, N., Debnath, A., and Sen, A.: Measurement of the effects of pH on phosphate availability, Plant Soil, 454, 217–224, https://doi.org/10.1007/s11104-020-04647-5, 2020.

Barré, P., Durand, H., Chenu, C., Meunier, P., Montagne, D., Castel, G., Billiou, D., Soucémarianadin, L., and Cécillon, L.: Geological control of soil organic carbon and nitrogen stocks at the landscape scale, Geoderma, 285, 50–56, https://doi.org/10.1016/j.geoderma.2016.09.029, 2017.

Bascomb, C. L.: Distribution of Pyrophosphate-Extractable Iron and Organic Carbon in Soils of Various Groups, J. Soil Sci., 19, 251–268, https://doi.org/10.1111/j.1365-2389.1968.tb01538.x, 1968.

Bassin, S., Volk, M., and Fuhrer, J.: Species Composition of Subalpine Grassland is Sensitive to Nitrogen Deposition, but Not to Ozone, After Seven Years of Treatment, Ecosyst., 16, 1105–1117, https://doi.org/10.1007/s10021-013-9670-3, 2013.

Blume, H.-P., Brümmer, G. W., Fleige, H., Horn, R., Kandeler, E., Kögel-Knaber, I., Kretzschmar, R., Stahr, K., and Wilke, B.-M.: Scheffer-/Schachtschabel Soil Science, Springer, Berlin Heidelberg, ISBN 978-3-642-30941-0, 10.1007/978-3-642-30942-7, 2016.

Brady, C., N. and Weil, R.: The Nature and Properties of Soils, Pearson, New Jersey, 14 edn., ISBN 978-0-13-227938-3, 2008.

Breiman, L.: Random Forests, Mach. Learn., 45, 5–32, https://doi.org/10.1023/A:1010933404324, 2001.

Brust, G. E.: Chapter 9: Management Strategies for Organic Vegetable Fertility, in: Safety and Practice for Organic Food, edited by Biswas, D. and Micallef, S., pp. 193–212, Academic Press, Cambridge, 2019.

Canedoli, C., Ferrè, C., Abu El Khair, D., Comolli, R., Liga, C., Mazzucchelli, F., Proietto, A., Rota, N., Colombo, G., Bassano, B., Viterbi, R., and Padoa-Schioppa, E.: Evaluation of ecosystem services in a protected mountain area: Soil organic carbon stock and biodiversity in alpine forests and grasslands, Ecosyst. Serv., 44, 101 135, https://doi.org/10.1016/j.ecoser.2020.101135, 2020.

Cao, Y.-Z., Wang, X.-D., Lu, X.-Y., Yan, Y., and Fan, J.-h.: Soil organic carbon and nutrients along an alpine grassland transect across Northern Tibet, J. Mt. Sci., 10, 564–573, https://doi.org/10.1007/s11629-012-2431-5, 2013.

Carlson, B. Z., Corona, M. C., Dentant, C., Bonet, R., Thuiller, W., and Choler, P.: Observed long-term greening of alpine vegetation—a case study in the French Alps, Environ. Res. Lett., 12, 114 006, https://doi.org/10.1088/1748-9326/aa84bd, 2017.

Carter, M. and Gregorich, E., eds.: Soil sampling and Methods of Analysis, CRC Press, Boca Raton, FL, USA, 2 edn., 2008.

Chen, L., Fang, K., Wei, B., Qin, S., Feng, X., Hu, T., Ji, C., and Yang, Y.: Soil carbon persistence governed by plant input and mineral protection at regional and global scales, Ecol. Lett., 24, 1018–1028, https://doi.org/10.1111/ele.13723, 2021.

Chen, S., Zhu, Y., Shao, T., Long, X., Gao, X., and Zhou, Z.: Relationship between rhizosphere soil properties and disease severity in highbush blueberry (Vaccinium corymbosum), Appl. Soil Ecol., 137, 187–194, https://doi.org/10.1016/j.apsoil.2019.02.015, 2019.

Choler, P., Bayle, A., Carlson, B. Z., Randin, C., Filippa, G., and Cremonese, E.: The tempo of greening in the European Alps: Spatial variations on a common theme, Glob. Change Biol., 27, 5614–5628, https://doi.org/10.1111/gcb.15820, 2021.

https://doi.org/10.5194/egusphere-2025-2006
Preprint. Discussion started: 14 May 2025

Currie, W. S.: Relationships between carbon turnover and bioavailable energy fluxes in two temperate forest soils, Glob. Change Biol., 9, 919–929, https://doi.org/https://doi.org/10.1046/j.1365-2486.2003.00637.x, 2003.

Daghino, S., Martino, E., Voyron, S., and Perotto, S.: Metabarcoding of fungal assemblages in Vaccinium myrtillus endosphere suggests colonization of above-ground organs by some ericoid mycorrhizal and DSE fungi, Sci. Rep., 12, 11 013, https://doi.org/10.1038/s41598-022-15154-1, 2022.

Dahlgren, R.: Quantification of Allophane and Imogolite, in: Quantitative Methods in Soil Mineralogy, p. 430, SSSA Miscellaneous Publication, Madison, WI, 1994.

Doetterl, S., Stevens, A., Six, J., Merckx, R., Van Oost, K., Casanova Pinto, M., Casanova-Katny, A., Muñoz, C., Boudin, M., Zagal Venegas, E., and Boeckx, P.: Soil carbon storage controlled by interactions between geochemistry and climate, Nature Geoscience, 8, 780–783, https://doi.org/10.1038/ngeo2516, 2015.

Doetterl, S., Berhe, A., Arnold, C., Bodé, S., Fiener, P., Finke, P., Fuchslueger, L., Griepentrog, M., Harden, J., Nadeu, E., Schnecker, J., Six, J., Trumbore, S., Oost, K., Vogel, C., and Boeckx, P.: Links among warming, carbon and microbial dynamics mediated by soil mineral weathering, Nature Geosci., 11, https://doi.org/10.1038/s41561-018-0168-7, 2018.

Duiker, S. W., Rhoton, F. E., Torrent, J., Smeck, N. E., and Lal, R.: Iron (Hydr)Oxide Crystallinity Effects on Soil Aggregation, SSSAJ, 67, 606–611, https://doi.org/10.2136/sssaj2003.6060, 2003.

Eckelmann, W., Sponagel, H., Grottenthaler, W., Hartmann, K.-J., Hartwich, R., Janetzko, P., Joisten, H., Kühn, D., Sabel, K.-J., and Traidl, R.: Bodenkundliche Kartieranleitung. KA5, Schweizerbart Science Publishers, Hannover, ISBN 978-3-510-95920-4, 2006.

Fang, K., Chen, L., Qin, S., Zhang, Q., Liu, X., Chen, P., and Yang, Y.: Mineral and Climatic Controls Over Soil Organic Matter Stability Across the Tibetan Alpine Permafrost Region, Global Biogeochem. Cycles, 35, e2021GB007 118, https://doi.org/10.1029/2021GB007118, 2021.

Federal Institute of Geosciences and Natural Resources: Geological Map of Germany, www.bgr.bund.de, 2020.

Federal Office of Topography swisstopo: Geological Map of Switzerland, www.swisstopo.admin.ch, 2020.

Guidi, C., Gosheva-Oney, S., Didion, M., Flury, R., Walthert, L., Zimmermann, S., Oney, B. J., Niklaus, P. A., Thürig, E., Viskari, T., Liski, J., and Hagedorn, F.: Drivers of soil organic carbon from temperate to alpine forests: a model-based analysis of the Swiss forest soil inventory with Yasso20, EGUsphere [preprint], pp. 1–26, https://doi.org/10.5194/egusphere-2024-3788, 2024.

Hagedorn, F., Mulder, J., and Jandl, R.: Mountain soils under a changing climate and land-use, Biogeochemistry, 97, 1–5, https://doi.org/10.1007/s10533-009-9386-9, 2010.

Hagedorn, F., Gavazov, K., and Alexander, J. M.: Above- and belowground linkages shape responses of mountain vegetation to climate change, Science, 365, 1119–1123, https://doi.org/10.1126/science.aax4737, 2019.

Haghipour, N., Ausin, B., Usman, M. O., Ishikawa, N., Wacker, L., Welte, C., Ueda, K., and Eglinton, T. I.: Compound-Specific Radiocarbon Analysis by Elemental Analyzer–Accelerator Mass Spectrometry: Precision and Limitations, Anal. Chem., 91, 2042–2049, https://doi.org/10.1021/acs.analchem.8b04491, 2019.

Hall, S. J. and Thompson, A.: What do relationships between extractable metals and soil organic carbon concentrations mean?, SSSAJ, 86, 195–208, https://doi.org/10.1002/saj2.20343, 2022.

Havlin, L., J., Tisdale, S., Beaton, J., and Nelson, W.: Soil Fertility and Fertilizers: An Introduction to Nutrient Management, Pearson, Chennai, Delhi, 8 edn., ISBN 978-0-13-503373-9, 2013.

Hendershot, W. H. and Duquette, M.: A Simple Barium Chloride Method for Determining Cation Exchange Capacity and Exchangeable Cations, SSSAJ, 50, 605–608, https://doi.org/10.2136/sssaj1986.03615995005000030013x, 1986.

https://doi.org/10.5194/egusphere-2025-2006
Preprint. Discussion started: 14 May 2025

Hitz, C., Egli, M., and Fitze, P.: Below-ground and above-ground production of vegetational organic matter along a climosequence in alpine grasslands, J. Plant Nutr. Soil Sci., pp. 389–397, https://doi.org/https://doi.org/10.1002/1522-2624(200108)164:4<389::AID-JPLN389>3.0.CO;2-A, 2001.

Jenny, H.: Factors of soil formation: a system of quantitative pedology, Dover Publications Inc., New York, ISBN 978-0-486-68128-3, 1994.

Jiang, J., Yang, Z., Liu, C., Zhu, H., Zhang, H., Yang, H., and Li, L.: Vaccinium corymbosum interact with mycorrhizal fungi to affect nitrogen metabolism and alleviate soil nutrient limitation, Appl. Soil Ecol., 204, 105 713, https://doi.org/10.1016/j.apsoil.2024.105713, 2024.

Kaiser, M., Zederer, D. P., Ellerbrock, R. H., Sommer, M., and Ludwig, B.: Effects of mineral characteristics on content, composition, and stability of organic matter fractions separated from seven forest topsoils of different pedogenesis, Geoderma, 263, 1–7, https://doi.org/10.1016/j.geoderma.2015.08.029, 2016.

Kirsten, M., Mikutta, R., Kimaro, D. N., Feger, K.-H., and Kalbitz, K.: Aluminous clay and pedogenic Fe oxides modulate aggregation and related carbon contents in soils of the humid tropics, SOIL, 7, 363–375, https://doi.org/10.5194/soil-7-363-2021, 2021.

Kleber, M., Eusterhues, K., Keiluweit, M., Mikutta, C., Mikutta, R., and Nico, P. S.: Chapter One - Mineral–Organic Associations: Formation, Properties, and Relevance in Soil Environments, in: Advances in Agronomy, edited by Sparks, D. L., pp. 1–140, Academic Press, https://doi.org/10.1016/bs.agron.2014.10.005, 2015.

Komada, T., Anderson, M. R., and Dorfmeier, C. L.: Carbonate removal from coastal sediments for the determination of organic carbon and its isotopic signatures, δ13C and Δ14C: comparison of fumigation and direct acidification by hydrochloric acid, L&O Methods, 6, 254–262, https://doi.org/10.4319/lom.2008.6.254, 2008.

Kuhn, M.: Building Predictive Models in R Using the caret Package, J. Stat. Softw., 28, 1–26, https://doi.org/10.18637/jss.v028.i05, 2008.

Kuhn, M. and Johnson, K.: Applied Predictive Modeling, Springer, New York, NY, ISBN 978-1-4614-6848-6, 2013.

Kögel-Knabner, I. and Kleber, M.: Mineralogical, Physicochemical, and Microbiological Controls on Soil Organic Matter Stabilization and Turnover, in: Handbook of Soil Sciences, edited by Huang, P. M., Li, Y., and Sumner, M. E., pp. 160–181, CRC Press, ISBN 978-0-429-09599-3, 2011.

Körner, C.: Alpine Plant Life: Functional Plant Ecology of High Mountain Ecosystems, Springer, 2 edn., 2003.

Küfmann, C.: Flugstaubeintrag und Bodenbildung im Karst der Nördlichen Kalkalpen, Nationalparkverwaltung Berchtesgaden, Berchtesgaden, Germany, ISBN 3-922325-61-0, 2008.

Leifeld, J., Zimmermann, M., Fuhrer, J., and Conen, F.: Storage and turnover of carbon in grassland soils along an elevation gradient in the Swiss Alps, Glob. Change Biol., 15, 668–679, https://doi.org/10.1111/j.1365-2486.2008.01782.x, 2009.

Li, H., Shen, H., Chen, L., Liu, T., Hu, H., Zhao, X., Zhou, L., Zhang, P., and Fang, J.: Effects of shrub encroachment on soil organic carbon in global grasslands, Sci. Rep., 6, 28 974, https://doi.org/10.1038/srep28974, 2016.

Liang, X., Yuan, J., Yang, E., and Meng, J.: Responses of soil organic carbon decomposition and microbial community to the addition of plant residues with different C:N ratio, Eur. J. Soil Biol., 82, 50–55, https://doi.org/10.1016/j.ejsobi.2017.08.005, 2017.

Lützow, M. v., Kögel-Knaber, I., Ekschmitt, K., Matzner, E., Guggenberger, G., Marschner, B., and Flessa, H.: Stabilization of organic matter in temperate soils: mechanisms and their relevance under different soil conditions – a review, Eur. J. Soil Sci., 57, 426–445, https://doi.org/https://doi.org/10.1111/j.1365-2389.2006.00809.x, 2006.

Mao, X., Van Zwieten, L., Zhang, M., Qiu, Z., Yao, Y., and Wang, H.: Soil parent material controls organic matter stocks and retention patterns in subtropical China, J. Soils Sediments, 20, https://doi.org/10.1007/s11368-020-02578-3, 2020.

https://doi.org/10.5194/egusphere-2025-2006
Preprint. Discussion started: 14 May 2025

Mathieu, J. A., Hatté, C., Balesdent, J., and Parent, E.: Deep soil carbon dynamics are driven more by soil type than by climate: a worldwide meta-analysis of radiocarbon profiles, Glob. Chang. Biol., 21, 4278–4292, https://doi.org/10.1111/gcb.13012, 2015.

Mehra, O. P. and Jackson, M. L.: Iron Oxide Removal from Soils and Clays by a Dithionite-Citrate System Buffered with Sodium Bicarbonate, Clays Clay Miner., 7, 317–327, https://doi.org/10.1346/CCMN.1958.0070122, 1958.

Miller, B. A. and Schaetzl, R. J.: Precision of Soil Particle Size Analysis using Laser Diffractometry, SSSAJ, 76, 1719–1727, https://doi.org/10.2136/sssaj2011.0303, 2012.

Muñoz, E., Chanca, I., and Sierra, C. A.: Increased atmospheric CO2 and the transit time of carbon in terrestrial ecosystems, Glob. Change Biol., 29, 6441–6452, https://doi.org/10.1111/gcb.16961, 2023.

Myrold, D. and Bottomley, P.: Nitrogen Mineralization and Immobilization, in: Nitrogen in Agricultural Systems, edited by Schepers, S. and Raun, W., Agronomy Monographs, p. 968, American Society of Agronomy, Crop Science Society of America, Soil Science Society of America, ISBN 978-0-89118-164-4, 2008.

Möhl, P., Mörsdorf, M. A., Dawes, M. A., Hagedorn, F., Bebi, P., Viglietti, D., Freppaz, M., Wipf, S., Körner, C., Thomas, F. M., and Rixen, C.: Twelve years of low nutrient input stimulates growth of trees and dwarf shrubs in the treeline ecotone, J. Ecol., 107, 768–780, https://doi.org/10.1111/1365-2745.13073, 2019.

Nie, X., Wang, D., Ren, L., Du, Y., and Zhou, G.: Storage and controlling factors of soil organic carbon in alpine wetlands and meadow across the Tibetan Plateau, Eur. J. of Soil Sci., 74, e13 383, https://doi.org/10.1111/ejss.13383, 2023.

Nomoto, H. A. and Alexander, J. M.: Drivers of local extinction risk in alpine plants under warming climate, Ecol. Lett., 24, 1157–1166, https://doi.org/10.1111/ele.13727, 2021.

Olagoke, F. K., Bettermann, A., Nguyen, P. T. B., Redmile-Gordon, M., Babin, D., Smalla, K., Nesme, J., Sørensen, S. J., Kalbitz, K., and Vogel, C.: Importance of substrate quality and clay content on microbial extracellular polymeric substances production and aggregate stability in soils, Biol. Fertil. Soils, 58, 435–457, https://doi.org/10.1007/s00374-022-01632-1, 2022.

O'Sullivan, M., Smith, W. K., Sitch, S., Friedlingstein, P., Arora, V. K., Haverd, V., Jain, A. K., Kato, E., Kautz, M., Lombardozzi, D., Nabel, J. E. M. S., Tian, H., Vuichard, N., Wiltshire, A., Zhu, D., and Buermann, W.: Climate-Driven Variability and Trends in Plant Productivity Over Recent Decades Based on Three Global Products, Global Biogeochem. Cycles, 34, e2020GB006 613, https://doi.org/10.1029/2020GB006613, 2020.

Paoli, G. D., Curran, L. M., and Slik, J. W. F.: Soil nutrients affect spatial patterns of aboveground biomass and emergent tree density in southwestern Borneo, Oecologia, 155, 287–299, https://doi.org/10.1007/s00442-007-0906-9, 2008.

Pepin, N., Bradley, R. S., Diaz, H. F., Baraer, M., Caceres, E. B., Forsythe, N., Fowler, H., Greenwood, G., Hashmi, M. Z., Liu, X. D., Miller, J. R., Ning, L., Ohmura, A., Palazzi, E., Rangwala, I., Schöner, W., Severskiy, I., Shahgedanova, M., Wang, M. B., Williamson, S. N., Yang, D. Q., and Mountain Research Initiative EDW Working Group: Elevation-dependent warming in mountain regions of the world, Nature Clim. Change, 5, 424–430, https://doi.org/10.1038/nclimate2563, 2015.

Percival, H. J., Parfitt, R. L., and Scott, N. A.: Factors Controlling Soil Carbon Levels in New Zealand Grasslands Is Clay Content Important?, SSSAJ, 64, 1623–1630, https://doi.org/10.2136/sssaj2000.6451623x, 2000.

Pignatti, E. and Pignatti, S.: Plant Life of the Dolomites: Vegetation Structure and Ecology, Springer, Berlin, Heidelberg, ISBN 978-3-642-31042-3, 2014.

Poeplau, C., Vos, C., and Don, A.: Soil organic carbon stocks are systematically overestimated by misuse of the parameters bulk density and rock fragment content, SOIL, 3, 61–66, https://doi.org/10.5194/soil-3-61-2017, 2017.

https://doi.org/10.5194/egusphere-2025-2006
Preprint. Discussion started: 14 May 2025

Püschel, D., Bitterlich, M., Rydlová, J., and Jansa, J.: Drought accentuates the role of mycorrhiza in phosphorus uptake, Soil Biol Biochem., 157, 108 243, https://doi.org/10.1016/j.soilbio.2021.108243, 2021.

Rasmussen, C., Heckman, K., Wieder, W. R., Keiluweit, M., Lawrence, C. R., Berhe, A. A., Blankinship, J. C., Crow, S. E., Druhan, J. L., Hicks Pries, C. E., Marin-Spiotta, E., Plante, A. F., Schädel, C., Schimel, J. P., Sierra, C. A., Thompson, A., and Wagai, R.: Beyond clay: towards an improved set of variables for predicting soil organic matter content, Biogeochemistry, 137, 297–306, https://doi.org/10.1007/s10533-018-0424-3, 2018.

Reichenbach, M., Fiener, P., Garland, G., Griepentrog, M., Six, J., and Doetterl, S.: The role of geochemistry in organic carbon stabilization in tropical rainforest soils, SOIL, 7, 453–475, https://doi.org/10.5194/soil-7-453-2021, 2021.

Reimer, P. J., Brown, T., and Reimer, R.: Discussion: Reporting and calibration of post-bomb 14C data, Tech. Rep. UCRL-JRNL-207168, Lawrence Livermore National Laboratory, Livermore, 2004.

Rennert, T.: Wet-chemical extractions to characterise pedogenic Al and Fe species – a critical review, Soil Res., 57, 1–16, https://doi.org/10.1071/SR18299, 2018.

Rowley, M. C., Grand, S., and Verrecchia, E. P.: Calcium-mediated stabilisation of soil organic carbon, Biogeochemistry, 137, 27–49, https://doi.org/10.1007/s10533-017-0410-1, 2018.

Rowley, M. C., Grand, S., Spangenberg, J. E., and Verrecchia, E. P.: Evidence linking calcium to increased organo-mineral association in soils, Biogeochemistry, 153, 223–241, https://doi.org/10.1007/s10533-021-00779-7, 2021.

Rumpf, S. B., Gravey, M., Brönnimann, O., Luoto, M., Cianfrani, C., Mariethoz, G., and Guisan, A.: From white to green: Snow cover loss and increased vegetation productivity in the European Alps, Science, 376, 1119–1122, https://doi.org/10.1126/science.abn6697, 2022.

Salomé, C., Nunan, N., Pouteau, V., Lerch, T. Z., and Chenu, C.: Carbon dynamics in topsoil and in subsoil may be controlled by different regulatory mechanisms, Glob. Change Biol., 16, 416–426, https://doi.org/10.1111/j.1365-2486.2009.01884.x, 2010.

Six, J., Paustian, K., Elliott, E. T., and Combrink, C.: Soil Structure and Organic Matter I. Distribution of Aggregate-Size Classes and Aggregate-Associated Carbon, SSSAJ, 64, 681–689, https://doi.org/10.2136/sssaj2000.642681x, _eprint: https://onlinelibrary.wiley.com/doi/pdf/10.2136/sssaj2000.642681x, 2000.

Six, J., Conant, R. T., Paul, E. A., and Paustian, K.: Stabilization mechanisms of soil organic matter: Implications for C-saturation of soils, Plant Soil, 241, 155–176, https://doi.org/10.1023/A:1016125726789, 2002.

Solly, E. F., Weber, V., Zimmermann, S., Walthert, L., Hagedorn, F., and Schmidt, M. W. I.: A Critical Evaluation of the Relationship Between the Effective Cation Exchange Capacity and Soil Organic Carbon Content in Swiss Forest Soils, Front. For. Glob. Change, 3, https://doi.org/10.3389/ffgc.2020.00098, 2020.

Steinbauer, M. J., Grytnes, J.-A., Jurasinski, G., Kulonen, A., Lenoir, J., Pauli, H., Rixen, C., Winkler, M., Bardy-Durchhalter, M., Barni, E., Bjorkman, A. D., Breiner, F. T., Burg, S., Czortek, P., Dawes, M. A., Delimat, A., Dullinger, S., Erschbamer, B., Felde, V. A., Fernández-Arberas, O., Fossheim, K. F., Gómez-García, D., Georges, D., Grindrud, E. T., Haider, S., Haugum, S. V., Henriksen, H., Herreros, M. J., Jaroszewicz, B., Jaroszynska, F., Kanka, R., Kapfer, J., Klanderud, K., Kühn, I., Lamprecht, A., Matteodo, M., di Cella, U. M., Normand, S., Odland, A., Olsen, S. L., Palacio, S., Petey, M., Piscová, V., Sedlakova, B., Steinbauer, K., Stöckli, V., Svenning, J.-C., Teppa, G., Theurillat, J.-P., Vittoz, P., Woodin, S. J., Zimmermann, N. E., and Wipf, S.: Accelerated increase in plant species richness on mountain summits is linked to warming, Nature, 556, 231–234, https://doi.org/10.1038/s41586-018-0005-6, 2018.

Torn, M. S., Kleber, M., Zavaleta, E. S., Zhu, B., Field, C. B., and Trumbore, S. E.: A dual isotope approach to isolate soil carbon pools of different turnover times, Biogeosciences, 10, 8067–8081, https://doi.org/10.5194/bg-10-8067-2013, 2013.

https://doi.org/10.5194/egusphere-2025-2006
Preprint. Discussion started: 14 May 2025

Trumbore, S.: Age of Soil Organic Matter and Soil Respiration: Radiocarbon Constraints on Belowground C Dynamics, Ecol. Appl., 10, 399–411, https://doi.org/10.1890/1051-0761(2000)010[0399:AOSOMA]2.0.CO;2, 2000.

VAO (Virtual Alpine Observatory): European Alps Climate Data, Tech. rep., Bavarian State Ministry of the Environment and Consumer Protection, https://www.alpendac.eu/node/3, 2020.

Vitasse, Y., Ursenbacher, S., Klein, G., Bohnenstengel, T., Chittaro, Y., Delestrade, A., Monnerat, C., Rebetez, M., Rixen, C., Strebel, N., Schmidt, B. R., Wipf, S., Wohlgemuth, T., Yoccoz, N. G., and Lenoir, J.: Phenological and elevational shifts of plants, animals and fungi under climate change in the European Alps, Biol. Rev., 96, 1816–1835, https://doi.org/10.1111/brv.12727, 2021.

Vohník, M. and Réblová, M.: Fungi in hair roots of Vaccinium spp. (Ericaceae) growing on decomposing wood: colonization patterns, identity, and in vitro symbiotic potential, Mycorrhiza, 33, 69–86, https://doi.org/10.1007/s00572-023-01101-z, 2023.

von Fromm, S. F., Hoyt, A. M., Lange, M., Acquah, G. E., Aynekulu, E., Berhe, A. A., Haefele, S. M., McGrath, S. P., Shepherd, K. D., Sila, A. M., Six, J., Towett, E. K., Trumbore, S. E., Vågen, T.-G., Weullow, E., Winowiecki, L. A., and Doetterl, S.: Continental-scale controls on soil organic carbon across sub-Saharan Africa, SOIL, 7, 305–332, https://doi.org/10.5194/soil-7-305-2021, 2021.

Walthert, L., Graf, U., Kammer, A., Luster, J., Pezzotta, D., Zimmermann, S., and Hagedorn, F.: Determination of organic and inorganic carbon, δ13C, and nitrogen in soils containing carbonates after acid fumigation with HCl, JPNSS, 173, 207–216, https://doi.org/10.1002/jpln.200900158, 2010.

Wasner, D., Abramoff, R., Griepentrog, M., Venegas, E. Z., Boeckx, P., and Doetterl, S.: The Role of Climate, Mineralogy and Stable Aggregates for Soil Organic Carbon Dynamics Along a Geoclimatic Gradient, Global Biogeochem. Cycles, 38, e2023GB007 934, https://doi.org/10.1029/2023GB007934, 2024.

Webber, P. J. and May, D. E.: The Magnitude and Distribution of Belowground Plant Structures in the Alpine Tundra of Niwot Ridge, Colorado$_*$, Arct. Antarct. Alp. Res., 9, 157–174, https://doi.org/10.1080/00040851.1977.12003911, 1977.

Welte, C., Hendriks, L., Wacker, L., Haghipour, N., Eglinton, T. I., Günther, D., and Synal, H.-A.: Towards the limits: Analysis of microscale 14C samples using EA-AMS, Nucl. Instrum. Methods Phys. Res., B, 437, 66–74, https://doi.org/10.1016/j.nimb.2018.09.046, 2018.

WRB, I. W. G.: World Reference Base for Soil Resources 2014, update 2015 International soil classification system for naming soils and creating legends for soil maps. World Soil Resources Reports, Tech. Rep. 106, FAO, Rome, 2015.

Yang, S., Jansen, B., Kalbitz, K., Chunga Castro, F. O., van Hall, R. L., and Cammeraat, E. L. H.: Lithology controlled soil organic carbon stabilization in an alpine grassland of the Peruvian Andes, Environ. Earth Sci., 79, 66, https://doi.org/10.1007/s12665-019-8796-9, 2020.

Yu, W., Weintraub, S. R., and Hall, S. J.: Climatic and Geochemical Controls on Soil Carbon at the Continental Scale: Interactions and Thresholds, Global Biogeochemical Cycles, 35, e2020GB006 781, https://doi.org/10.1029/2020GB006781, 2021.

Zhang, X. and Wang, W.: The decomposition of fine and coarse roots: their global patterns and controlling factors, Sci. Rep., 5, 9940, https://doi.org/10.1038/srep09940, 2015.

Zhao, J., Yang, W., Ji-Shi, A., Ma, Y., Tian, L., Li, R., Huang, Z., Liu, Y.-F., Leite, P. A. M., Ding, L., and Wu, G.-L.: Shrub encroachment increases soil carbon and nitrogen stocks in alpine grassland ecosystems of the central Tibetan Plateau, Geoderma, 433, 116 468, https://doi.org/10.1016/j.geoderma.2023.116468, 2023.